NATIONAL ADVISORY COMMITTEE FOR AERONAUTICS

WARTIME REPORT

ORIGINALLY ISSUED

October 1945 as
Advance [redacted] Report L5H08

SUPERSONIC-TUNNEL TESTS OF PROJECTILES IN GERMANY AND ITALY

By Antonio Ferri

Langley Memorial Aeronautical Laboratory
Langley Field, Va.

WASHINGTON

NACA ACR No. L5H08

NATIONAL ADVISORY COMMITTEE FOR AERONAUTICS

ADVANCE [redacted] REPORT

SUPERSONIC-TUNNEL TESTS OF PROJECTILES IN GERMANY AND ITALY

By Antonio Ferri

SUMMARY

Tests were performed in the Göttingen (Germany) and Guidonia (Italy) supersonic tunnels in order to determine the aerodynamic characteristics of projectiles of various shapes. The Mach numbers ranged from about 1.3 to 3.2 for the Göttingen tests and from 1.44 to 2.66 for the Guidonia tests. The results show that increasing the relative length of the nose causes the drag coefficient to decrease and the center of pressure to move forward. For a given length, the nose having minimum drag has a curved profile; the curvature is greatest at the tip and decreases to a very small value toward the rear of the nose, where the shape becomes approximately conical. As the Mach number increases, the drag coefficient decreases and the center of pressure moves toward the tail. For the higher Mach numbers the variation of the drag coefficient and the movement of the center of pressure are small. Existing aerodynamic theory gives values of the aerodynamic characteristics close to those determined experimentally for small flow deviations.

INTRODUCTION

Research on projectiles was started at approximately the same time (1942) at the Göttingen Laboratory in Germany and the Guidonia Laboratory in Italy. The original data were brought to the United States in 1944 and were tabulated and analyzed at the Langley Memorial Aeronautical Laboratory of the National Advisory Committee for Aeronautics.

The aim of the German research was to determine the variation of aerodynamic characteristics with Mach number for various fundamental geometrical shapes for projectiles.

Force tests of small models 0.393 inch in diameter were conducted in a supersonic tunnel having a test section approximately 2.36 by 2.84 inches. The shape of the models was systematically varied to determine the effects on the aerodynamic characteristics of:

(1) Nose profile shape for a typical fineness ratio

(2) Nose length for noses with circular-arc profiles

(3) Small taper of the tail of the projectile

The program carried out at the Guidonia Laboratory had as its aim the development of an optimum shape for a 1.812-inch-caliber antitank projectile. Because of the relatively large size of the test model, it was possible to obtain pressure-distribution studies as well as precise aerodynamic data for comparison with results derived by existing theory.

The theories presented in references 1 to 6 for sharp-nose projectiles at zero angle of attack and the theories of references 7 and 8 for bodies of revolution at an angle of yaw were used to compute the theoretical characteristics of the various conical noses for comparison with the experimental results. The aerodynamic theory of minimum-drag projectiles presented in references 3 and 5 to 7 was used as a guide in the design of the various nose shapes of the projectiles tested.

SYMBOLS

The symbols used for defining the aerodynamic coefficients and the geometric characteristics of the projectiles are given in figure 1.

a_o speed of sound in free stream

V_o free-stream velocity

M_o free-stream Mach number (V_o/a_o)

q_o free-stream dynamic pressure

p local static pressure

[redacted]

p_o free-stream static pressure

P pressure coefficient $\left(\frac{p - p_o}{q_o}\right)$

d diameter of body of projectile

R resultant force on projectile

D drag

L lift

M pitching moment about rear face of projectile

C_D drag coefficient of model $\left(\frac{D}{q_o\left(\pi \frac{d^2}{4}\right)}\right)$

C_L lift coefficient of model $\left(\frac{L}{q_o\left(\pi \frac{d^2}{4}\right)}\right)$

C_m pitching-moment coefficient about rear face of projectile $\left(\frac{M}{q_o\left(\pi \frac{d^2}{4}\right)d}\right)$

l length of projectile

l_N length of nose of projectile

r radius of nose of projectile

f center-of-pressure position, measured from rear face of projectile

α angle of attack of projectile

n fineness ratio of projectile (l/d)

n_N fineness ratio of nose (l_N/d)

ϵ angle between intersection of tangent on nose of projectile and generatrix of cylinder

[redacted]

EXPERIMENTS AT GOTTINGEN

Wind-Tunnel and Experimental Methods

Experiments were carried out by German technicians of the Aerodynamische Versuchsanstalt (AVA) in the small supersonic tunnel at the Göttingen Laboratory. The layout of the wind tunnel is shown in figure 2. The tunnel has a rectangular section with a throat about 2.36 by 2.84 inches. As indicated in figure 2, a semiopen throat arrangement was used. The side walls of the tunnel were straight and parallel, but the jet was not restrained by top and bottom walls. It has been found that this arrangement makes it possible to obtain reliable aerodynamic data at Mach numbers only slightly greater than 1.0 (reference 9) and that the choking condition which would exist if the jet were completely restrained does not occur. Some trouble was encountered during the tests because of condensation phenomena, in spite of the fact that the humidity of the ambient air had been reduced to a low value by preliminary drying.

The tests consisted of the measurement of lift, drag, and pitching moment with a semiautomatic balance. Each model was tested through an angle-of-attack range from 9° to -3° and a Mach number range from 1.3 to 3.2. For the longer models, it was not possible to perform the tests at the low velocities because the front shock wave reflecting from the jet boundaries interfered with the flow on the rear face of the projectile.

Test Models

The models each had a diameter of 0.393 inch and were supported by a sting attached to the rear face. The dimensions of the sting and the tare system adopted are not known.

The models can be separated into three distinct groups to determine the effect of:

Nose shape.- Four projectiles having over-all fineness ratios n of 5.0 with nose fineness ratios of 2.5 (models 1, 2, 3, and 4, fig. 3) were tested to determine the effect of the nose shape. Because the models were small, they had no tail taper or bourrelet ring. All the noses

were of circular profile with the radii r varying from 6.5d to ∞ (conical nose). For the nose with 6.5d radius (model 1, fig. 3), the end of the nose was tangent to the cylinder at their juncture but, for the other models, the profile of the nose terminated with its tangent inclined at an angle ϵ with respect to the generatrix of the cylinder.

Length of the nose.- Five models having nose lengths varying from 0.5d to 3.5d (models 5, 6, 1, 7, and 8, fig. 4) were tested to determine the effect of the length of the nose. The noses of all the models had circular profiles tangent to the cylinder forming the body of the projectile.

Tail taper.- Three models derived from model 1 and having three different tail tapers (models 9, 10, and 11, fig. 5) were tested to determine the effect of tail taper.

Results

Wind-tunnel tests.- The results of the experiments at the Göttingen Laboratory are given in figures 6 to 21. Figures 6 to 11 show the results of tests to determine the effect of the nose shape. In figures 6 to 9 the variation of the aerodynamic coefficients for models 1, 2, 3, and 4 is shown for several angles of attack and a range of Mach numbers. Figures 10 and 11 show the aerodynamic coefficients of each projectile at equal Mach numbers as a function of the ratio d/r. As shown in figures 10 and 11, the minimum drag coefficient was obtained for a nose intermediate to the noses for which r = ∞ and r = 12.5d. The differences in the minimum drag coefficients were not large.

The results of the tests to determine the effect of the length of the nose are given in figures 12 to 17. Increasing the fineness ratio of the nose n_N caused the drag coefficient to drop noticeably (fig. 16). The slope dC_D/dn_N decreased as n_N increased. The center of pressure of the projectiles moved toward the nose as the fineness ratio of the nose increased (fig. 17).

The results of the tests to evaluate the effect of the tail taper are given in figures 18 to 21. The variation of the aerodynamic coefficients with Mach number is

[redacted]

shown in figures 18 to 20, and data for comparison of the tapered models with model 1 are shown in figure 21. The drag of the projectile was lowest for the longest tapered tail, especially at the lower Mach numbers (fig. 21). The differences in drag coefficients were not large. The other aerodynamic characteristics were not appreciably altered.

The drag coefficient for a given projectile shape decreased as the Mach number was increased. This effect was most pronounced at the lower supersonic velocities; the variation at Mach numbers of the order of 3.0 was slight. The position of the center of pressure did not change appreciably with angle of attack. In the lower supersonic velocity range the center of pressure moved toward the rear of the projectile as the speed was increased but tended to approach a fixed location at the higher Mach numbers.

Firing tests.- Actual firing tests were performed to verify the experimental values, and the following results were obtained:

Model	C_D	
	Firing tests ($\alpha \approx 3^\circ$)	Tunnel tests ($\alpha = 3^\circ$)
1	0.40	0.29
2	.36	.27
3	.35	.26
4	.40	.28

These results were for a Mach number of 2.2.

The projectiles used in the firing tests had an angle of attack of nearly 3° and a bourrelet ring. Drag coefficients obtained from firing tests at angles of attack near 3° gave drag coefficients that were equivalent to a wind-tunnel angle of attack of about 7.5°. The differences therefore cannot be entirely due to the presence of the bourrelet nor to the error in angle of attack. The differences may probably be attributed in part to the difference of surface finish between the tunnel model and the fired projectiles, the rotation of the fired projectile about its axis, and the difference in Reynolds number for the firing and the tunnel tests.

[redacted]

EXPERIMENTS AT GUIDONIA

Wind-Tunnel and Experimental Methods

Projectiles with nine different nose shapes were tested in the closed-throat high-speed tunnel at Guidonia (reference 10) at Mach numbers ranging from 1.44 to 2.66. The system of the partially open stream was not used because it required a larger amount of power and therefore limited the maximum velocity. The test section was large enough not to require special attention to prevent choking of the air stream with the model in the tunnel when the Mach number was greater than 1.44. The nozzles were of rectangular section of the two-dimensional type with a minimum section 15.74 by 15.74 inches.

The forces on each model were determined by use of a three-component balance (reference 10). The model was attached to the balances by a sting on the projectile axis on the rear face of the projectile. The sting, although of small diameter, affected the experimental results somewhat since it increased the pressure on the rear face of the projectile. It was necessary, therefore, to make an accurate tare measurement by suspending the model on a faired strut attached to the side of the projectile.

Pressure distributions and optical observations of the flow were also obtained for some of the projectiles tested. It was difficult to obtain good flow photographs because the phenomena were conical and the density of the air was extremely low. Some of the observations were made with a schlieren apparatus, and in some cases data were obtained by means of a shadowgraph apparatus.

Before the systematic experiments were started, the results obtained in the tunnel were compared with those obtained by firing tests. A sphere tested at two velocities (M_o = 2.06 and M_o = 2.62) had a constant drag coefficient (C_D = 0.93). These wind-tunnel results on the sphere at Guidonia agreed with the firing data (C_D = 0.96) and were close to the results obtained at Göttingen, for which the drag coefficient in the Mach number range between 1.3 and 3.1 was almost constant and equal to 1.01. In an earlier wind-tunnel experiment (reference 11), somewhat lower drag coefficients were

[redacted]

found: 0.87 for a Mach number of 1.85 and 0.86 for a Mach number of 2.13. These earlier results, however, are questionable because the effect of the support strut, which increases the pressure at the rear somewhat, was neglected.

Test Projectiles

A 1.812-inch-caliber antitank projectile was used for the body of the projectile in the Guidonia tests, the details of which are shown in figure 22. Nine different nose shapes (fig. 23) were tested with this body in order to determine the nose for minimum drag.

Conical noses of varying fineness ratio (projectiles 1, 2, 3, and 4 of fig. 23) were tested first in order to estimate the importance of fineness ratio. The simple conical nose form was chosen to permit comparison with existing theoretical data for conical noses.

Both the approximate projectile theories (references 4 and 5) and the complex but more exact theory of Ferrari (references 6, part II, and 7) show that, in order to minimize the drag of the projectile, it is necessary to concentrate the pressure at the vertex of the nose and then to carry out the most rapid expansion possible. With this criterion as a guide, five noses of fineness ratio $n_N = 2.0$ were designed (projectiles 5, 6, 7, 8, and 9 of fig. 23). (See table I.) Two of the noses tested, projectiles 8 and 9, were blunt-ended but were otherwise similar to the nose of projectile 5. The nose of projectile 5 approaches that theoretically derived by Ferrari (reference 6). A nose exactly corresponding with the optimum nose described by the theory of Ferrari was about to be tested when the tests were suspended.

Results

The results of the experiments at Guidonia are shown in figures 24 to 35. The variation of C_D and f/d with fineness ratio of the nose at a Mach number of 2.06 and an angle of attack of 0° is shown in figure 24; the variation of C_D and f/d with Mach number for the nose having a fineness ratio of 2.0 (projectile 3) at an angle of attack of 0° is shown in figure 25. The drag coefficient

[redacted]

for a given projectile shape decreased as the Mach number increased. The position of the center of pressure did not change appreciably with angle of attack. The values obtained from firing tests for two noses having fineness ratios of 2.0 and 2.5 at a Mach number of 2.14 are also shown in figure 24. The angle of attack in the firing tests varied between 2° and 3°.

The drag values given by the firing tests are somewhat higher than those determined in the wind tunnel. The difference can probably be attributed to the fact that the models in the tunnel were perfectly finished but the fired projectiles had a rough machine finish. The fired projectile also had a rotational motion that was not reproduced in the tunnel tests and that undoubtedly altered the phenomenon of the boundary layer.

The variation of the aerodynamic coefficients with angle of attack for projectiles 1 and 3 is shown in figure 26 for $M_0 = 2.06$. The values obtained from integration of the pressure distributions are also shown. The pressure distributions over projectiles 1 and 3 were determined at angles of attack of 0°, 4°, and 8°. When the projectile was yawed, the pressure was determined at seven stations around the projectile from 0° to 180°. The pressure distributions for projectiles 1 and 3 are shown in figures 27 and 28. In figure 29 flow photographs for zero angle of attack are shown for these projectiles.

The following tables show calculated values of the initial shock-wave angle and the pressure coefficient on the nose for projectiles 1 and 3 at a Mach number of 2.06. These quantities were calculated by the method of references 7 and 8. Experimental values of these quantities are shown for comparison.

Nose	Angle of shock wave (deg)	
	Theoretical	Experimental
$\alpha = 0°$		
1	44.5	46.0
3	33.0	33.2

[redacted]

Nose	Station (deg)	Pressure coefficient, $\frac{p - p_o}{q_o}$	
		Theoretical	Experimental
$\alpha = 0^\circ$			
1	-------	0.53	0.60
3	-------	.18	.19
$\alpha = 4^\circ$			
1	0	0.67	0.71
1	180	.40	.53
3	0	.27	.28
3	180	.11	.14
$\alpha = 8^\circ$			
1	0	0.83	0.84
1	180	.29	.43
3	0	.37	.36
3	180	.06	.08

The following observations can be made from these test results:

(1) When the flow deviations are small, the nose phenomena are close to those predicted by the theory.

(2) At the higher angles of yaw appreciable differences exist between the theoretical and experimental pressure coefficients, particularly if the nose is short.

(3) Pressure on the rear face of the projectile is only slightly affected by the nose shape but is appreciably decreased with an increase of angle of attack.

Figure 30 shows the variation of the aerodynamic coefficients with angle of attack for projectile 8, and figure 31 gives the pressure distributions for this projectile at a Mach number of 2.06. The following

[redacted]

table compares the drag coefficients for $\alpha = 0^\circ$ and the center-of-pressure positions for the various projectiles for $M_o = 2.06$:

Projectile	C_D	f/d
3	0.368	1.98
5	.352	2.03
6	.392	----
7	.376	----
8	.362	2.19
9	.358	2.09

It will be observed that projectiles 5, 8, and 9 had the lowest drag. These three shapes are closer to the optimum profile predicted theoretically than any of the other noses tested. The pressure-distribution diagrams (fig. 31) and the flow photographs (figs. 34 and 35) show that, when the front part of the projectile is flat as for projectiles 8 and 9, a normal shock wave occurs and the pressure at the nose approaches the stream total pressure in value. The shock wave is detached from the projectile. Immediately behind the blunt face of the nose a rapid expansion occurs, and the pressures a short distance from the nose become lower than for the conical nose. These lower pressures act over a relatively large part of the frontal area of the projectile; consequently, a lower drag coefficient is obtained for the blunt nose than for the conical nose. The pressure on the rear face of the projectile is about the same for both types of nose. The lift at the same angle of attack for the blunt noses is slightly greater than for the conical noses, and the center of pressure is therefore farther forward. These differences are very small, however. It may be mentioned that the blunt type of nose is more practical than the sharp-pointed nose from the standpoints of construction and maintenance.

CONCLUSIONS

Tests were performed in the Göttingen (Germany) and Guidonia (Italy) supersonic tunnels in order to determine the aerodynamic characteristics of projectiles of various

[redacted]

shapes. The following conclusions are based on the results of both the German and the Italian experiments:

1. The fineness ratio of the nose is of primary importance in determining the aerodynamic characteristics of supersonic projectiles. As the fineness ratio increases, the drag coefficient decreases and the center of pressure moves forward.

2. The drag coefficient for a given projectile shape decreases as the Mach number is increased. This effect is most pronounced at the lower supersonic velocities; the variation at Mach numbers of the order of 3.0 is slight.

3. The position of the center of pressure does not change appreciably with angle of attack. In the lower supersonic velocity range the center of pressure moves toward the rear of the projectile as the speed is increased but tends to approach a fixed location at the higher Mach numbers.

4. The pressure on the rear face of the projectile varies appreciably with angle of attack but is only slightly affected by the form of the nose.

5. For a given fineness ratio the optimum nose profile has a relatively blunt end, which is faired to the cylindrical part of the projectile. The theoretical criterions for the design of the optimum nose profile have been verified.

6. The existing aerodynamic theory for the calculation of the pressure distribution about projectiles is adequately precise for small flow deviations.

7. The addition of a small taper to the tail of the projectile diminishes the drag slightly, particularly at the lower Mach numbers, without altering the other aerodynamic characteristics.

Langley Memorial Aeronautical Laboratory
National Advisory Committee for Aeronautics
Langley Field, Va.

REFERENCES

1. Taylor, G. I., and Maccoll, J. W.: The Air Pressure on a Cone Moving at High Speeds. Proc. Roy. Soc. (London), ser. A, vol. 139, no. 838, Feb. 1, 1933, pp. 278-311.

2. Busemann, A.: Drücke auf kegelförmige Spitzen bei Bewegung mit Überschallgeschwindigkeit. Z.f.a.M.M., Bd. 9, Heft 6, Dec. 1929, pp. 496-498.

3. Ferrari, C.: Campo aerodinamico a velocità iper-acustica attorno a un solido di rivoluzione a prora acuminata. L'Aerotecnica, vol. XVI, no. 2, Feb. 1936, pp. 121-130.

4. von Kármán, Theodor, and Moore, Norton B.: Resistance of Slender Bodies Moving with Supersonic Velocities, with Special Reference to Projectiles. Trans. A.S.M.E., vol. 54, no. 23, Dec. 15, 1932, pp. 303-310.

5. von Kármán, Th.: The Problem of Resistance in Compressible Fluids. GALCIT Pub. No. 75, 1936. (From R. Accad. d'Italia, cl. sci. fis., mat. e nat., vol. XIV, 1936.)

6. Ferrari, C.: The Determination of the Projectile of Minimum Wave-Resistance. R.T.P. Translation No. 1180, British Ministry of Aircraft Production. (Part I from Atti R. Accad. Sci. Torino, vol. 74, July-Oct. 1939, pp. 675-693; Part II from Atti R. Accad. Sci. Torino, vol. 75, Nov.-Dec. 1939, pp. 61-96.)

7. Ferrari, C.: Campi di corrente ipersonora attorno a solidi di rivoluzione. L'Aerotecnica, vol. XVII, no. 6, June 1937, pp.507-518.

8. Ferrari, C.: Determination of the Pressure Exerted on Solid Bodies of Revolution with Pointed Noses Placed Obliquely in a Stream of Compressible Fluid at Supersonic Velocity. R.T.P. Translation No. 1105, British Ministry of Aircraft Production. (From Atti R. Accad. Sci. Torino, vol. 72, Nov.-Dec. 1936, pp. 140-163.)

[redacted]

9. Ferri, Antonio: Completed Tabulation in the United States of Tests of 24 Airfoils at High Mach Numbers (Derived from Interrupted Work at Guidonia, Italy, in the 1.31- by 1.74-Foot High-Speed Tunnel). NACA ACR No. L5E21, 1945.

10. Ferri, Antonio: La galleria ultrasonora di Guidonia. Atti di Guidonia No. 15, 1939. (Available in Aircraft Engineering, vol. XII, no. 140, Oct. 1940, pp. 302-305.)

11. Ferri, Antonio: Influenza del numero di Reynolds ai grandi numeri di Mach. Atti di Guidonia No. 67-68-69, 1942. (Available as R.T.P. Translation No. 1988, British Ministry of Aircraft Production.)

[redacted]

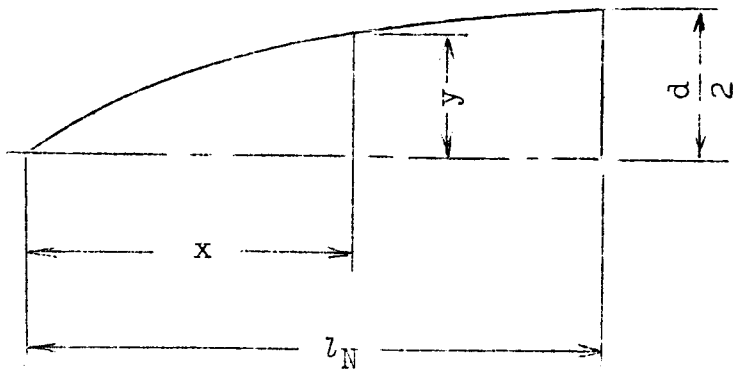

TABLE I

NOSE ORDINATES FOR PROJECTILES TESTED AT GUIDONIA

Projectile / x	y				
	5	6	7	8	9
0	0	0	0	0	0
.25	.1	.6	.2	2.5	1.3
.50	.2	.9	.3	2.7	1.5
1.00	.4	1.6	.6	3.2	1.6
2.00	1.0	2.9	2.0	3.7	2.1
3.00	1.4	4.1	2.4	4.0	2.5
5.00	2.2	5.7	3.8	4.6	3.3
10.00	3.9	8.9	6.7	6.3	5.1
20.00	7.5	14.0	11.4	9.2	8.9
30.00	10.9	17.9	14.9	12.3	12.3
40.00	14.1	20.7	17.6	15.1	15.4
50.00	17.1	22.5	19.9	17.7	17.9
60.00	19.7	23.8	21.7	19.8	19.9
70.00	21.5	24.5	23.0	21.5	21.5
80.00	23.0	24.9	23.9	23.0	23.0
90.00	24.2	25.0	24.5	24.2	24.2
100.00	25.0	25.0	25.0	25.0	25.0

NATIONAL ADVISORY
COMMITTEE FOR AERONAUTICS

[redacted]

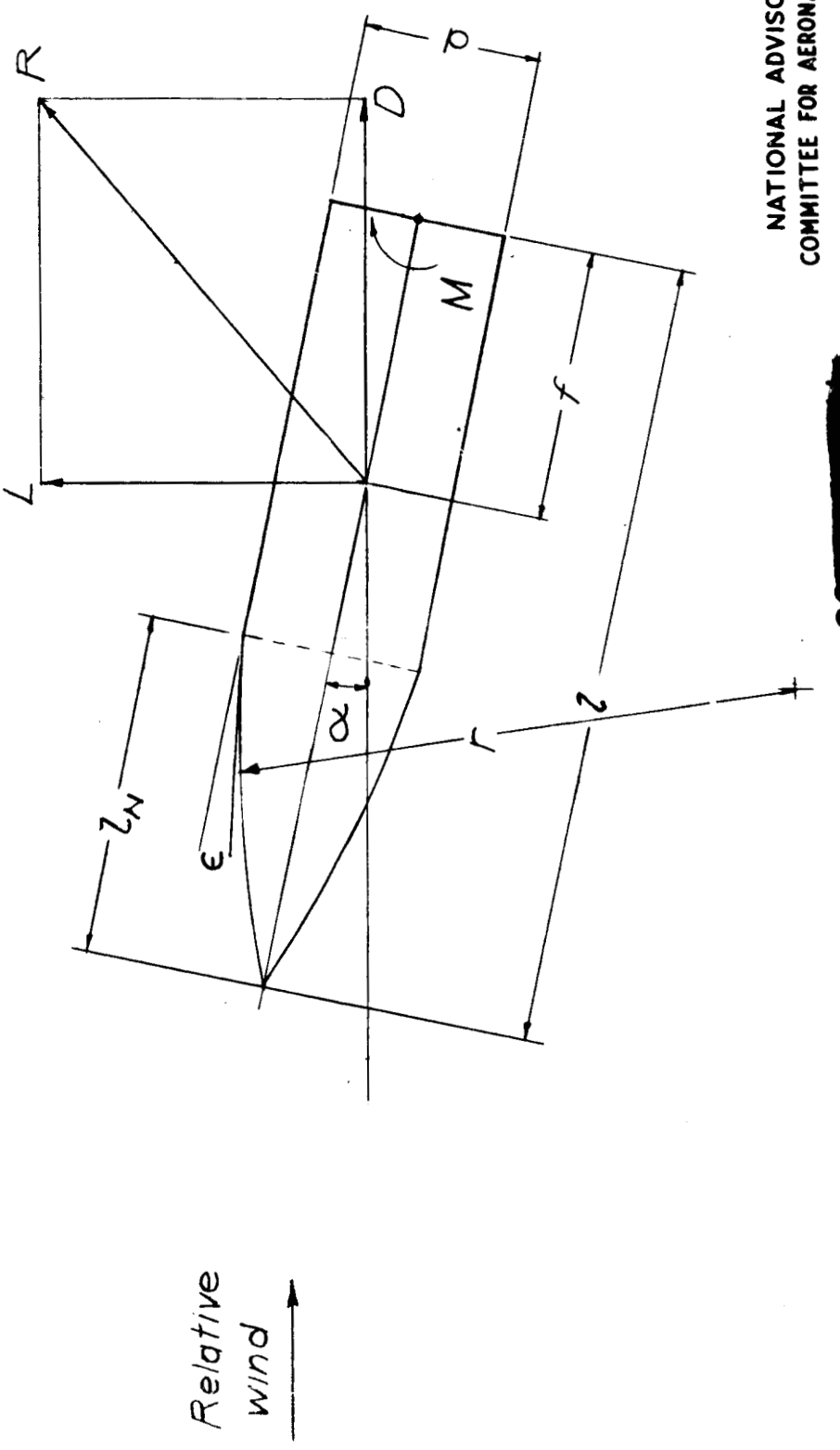

Figure 1.- Definition of symbols.

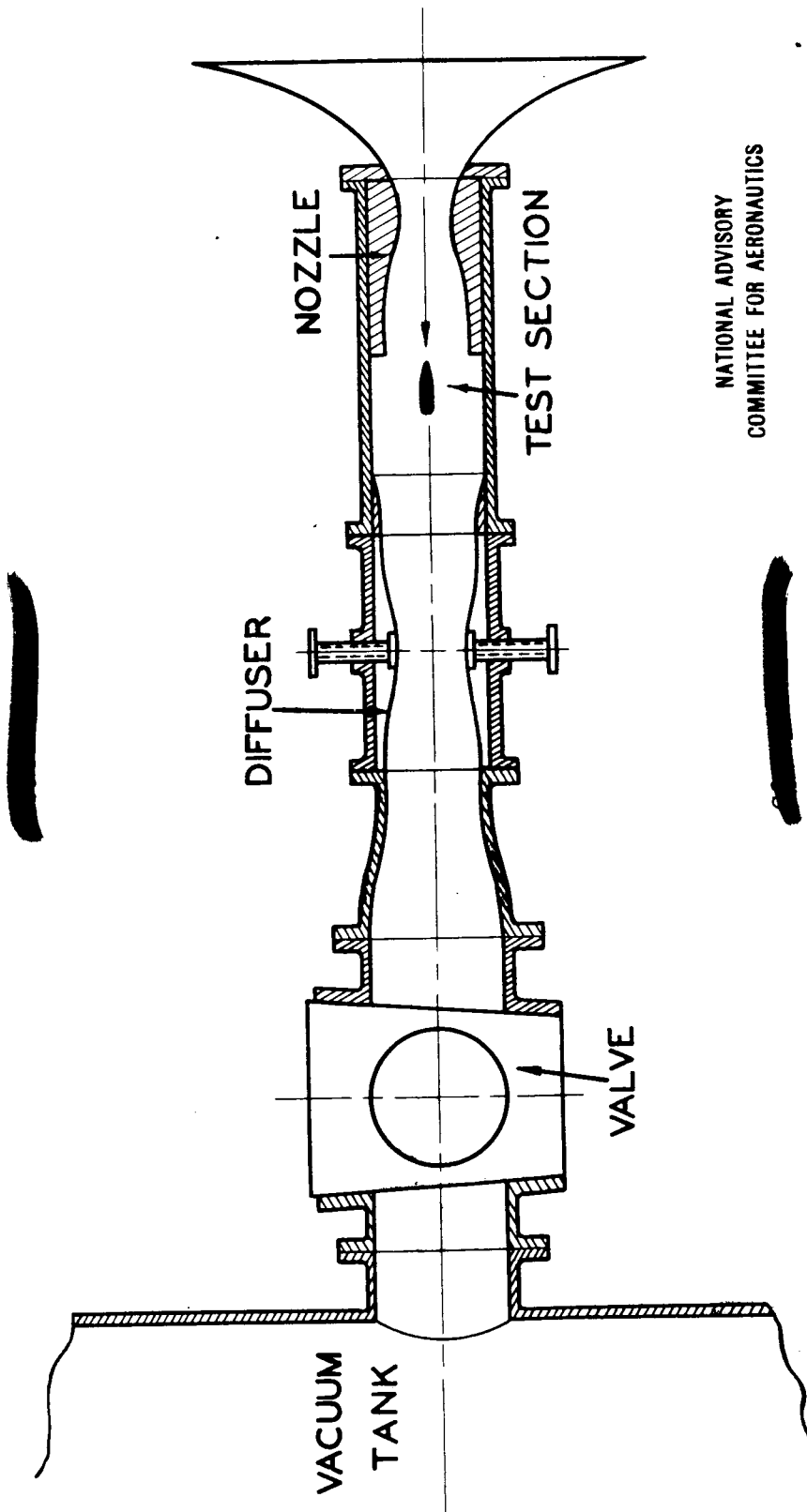

Figure 2.- The Göttingen supersonic tunnel.

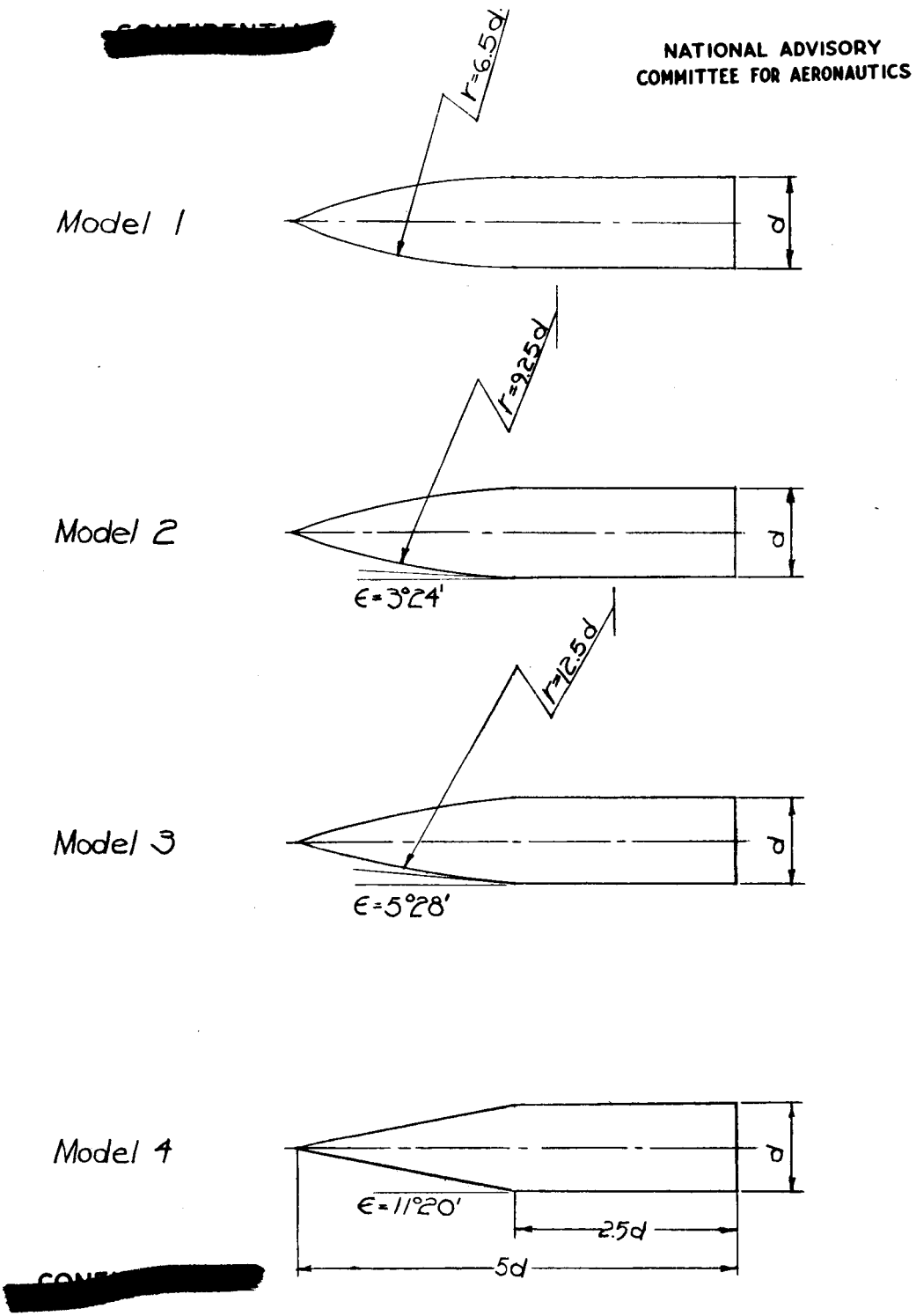

Figure 3.- Models tested at Göttingen to determine the nose of minimum drag. d = 0.393 inch.

[redacted]

NATIONAL ADVISORY
COMMITTEE FOR AERONAUTICS

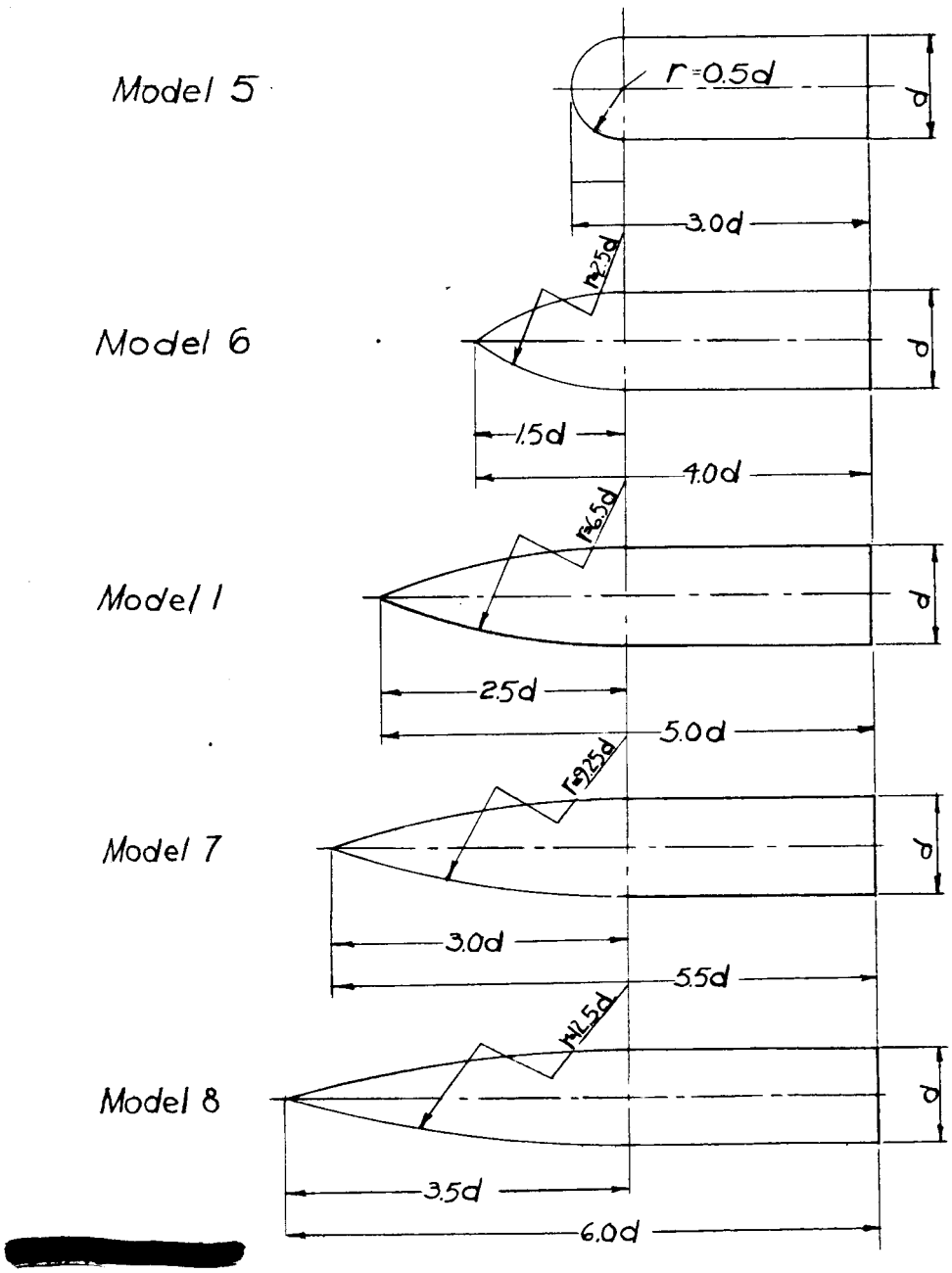

[redacted]

Figure 4.- Models tested at Göttingen to determine the effect of nose length. d = 0.393 inch.

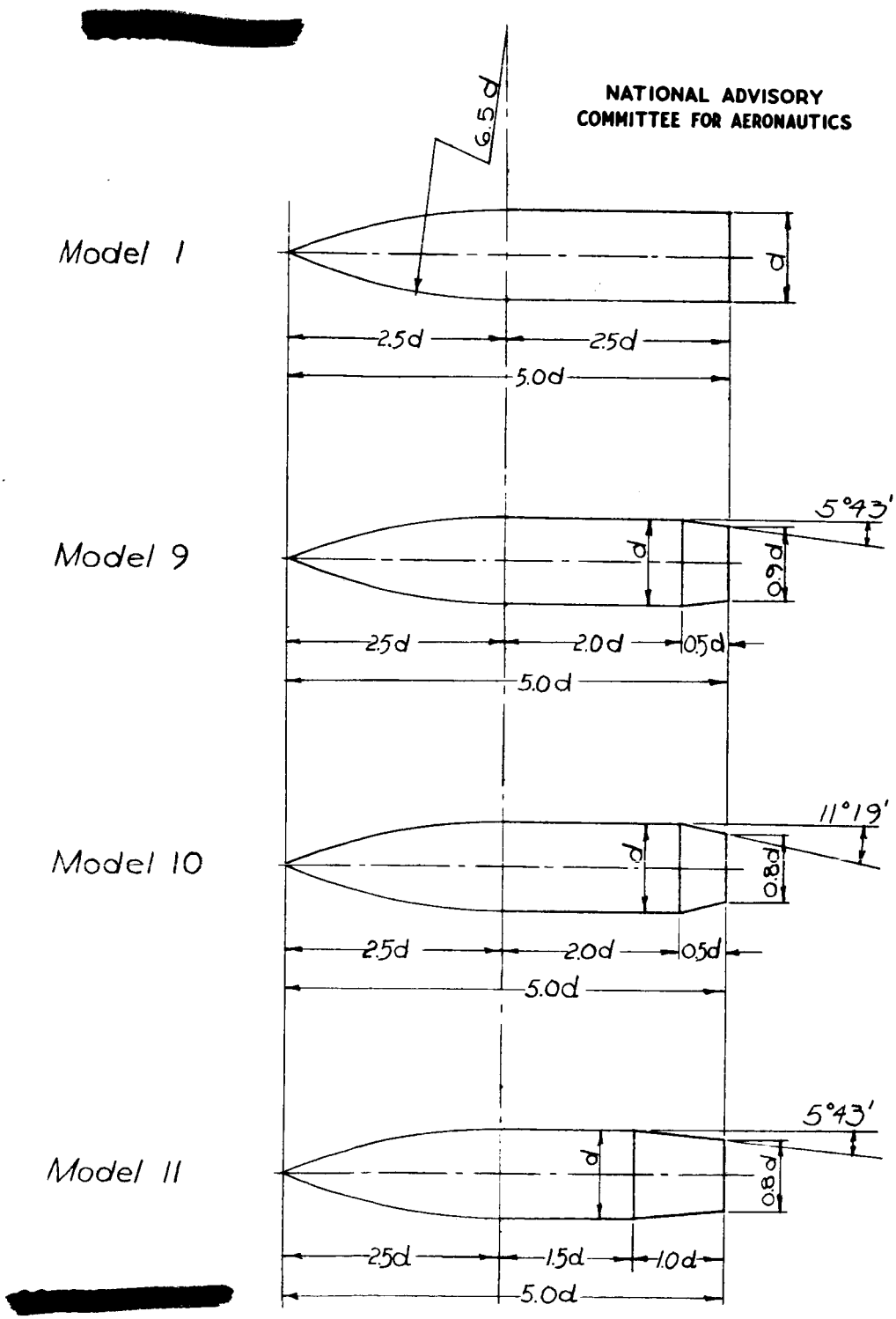

Figure 5.- Models tested at Göttingen to determine the effect of tail taper. d = 0.393 inch.

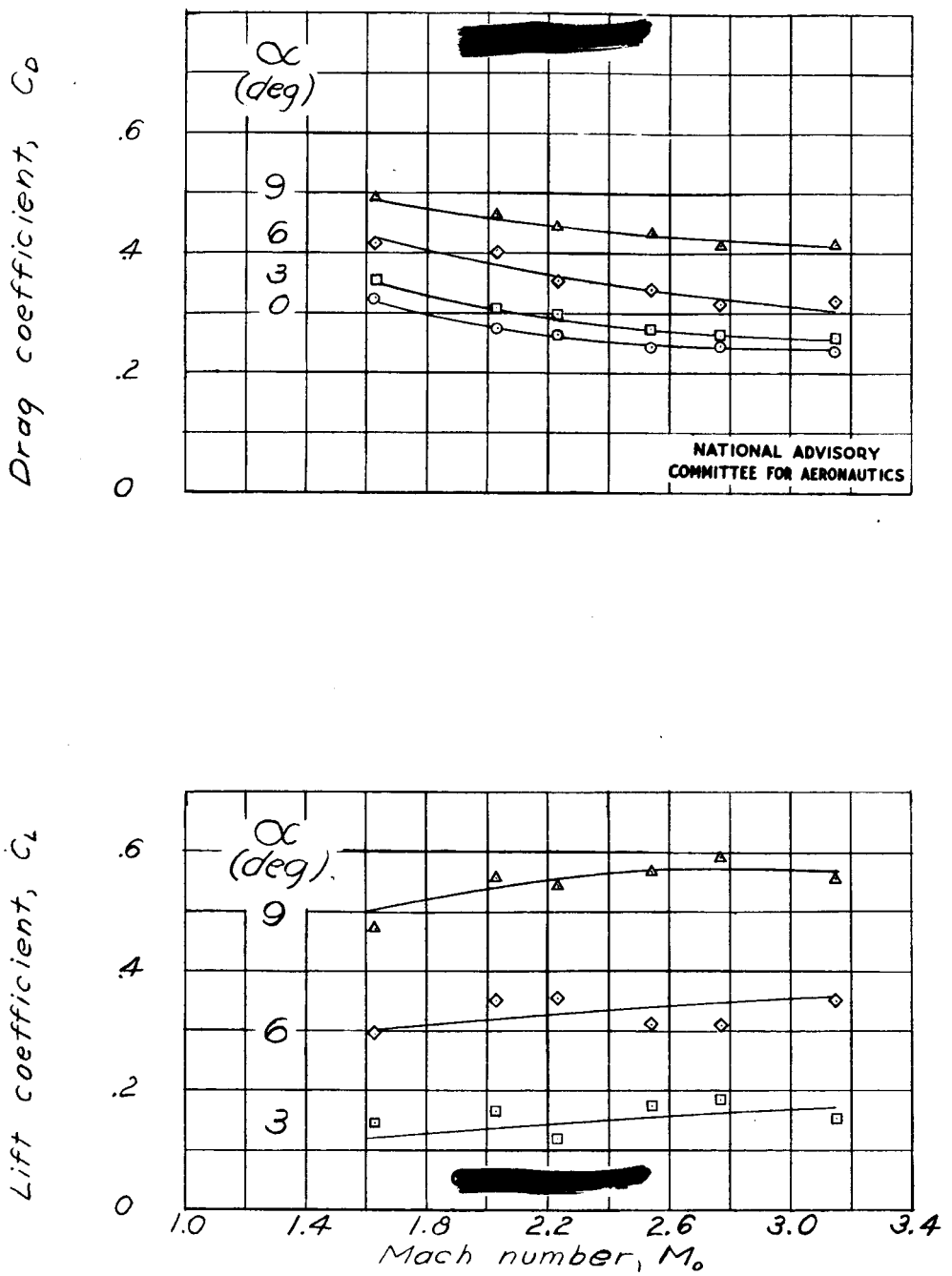

Figure 6.- Lift, drag, and moment coefficients and position of center of pressure as functions of Mach number for various angles of attack. Model 1. (Göttingen).

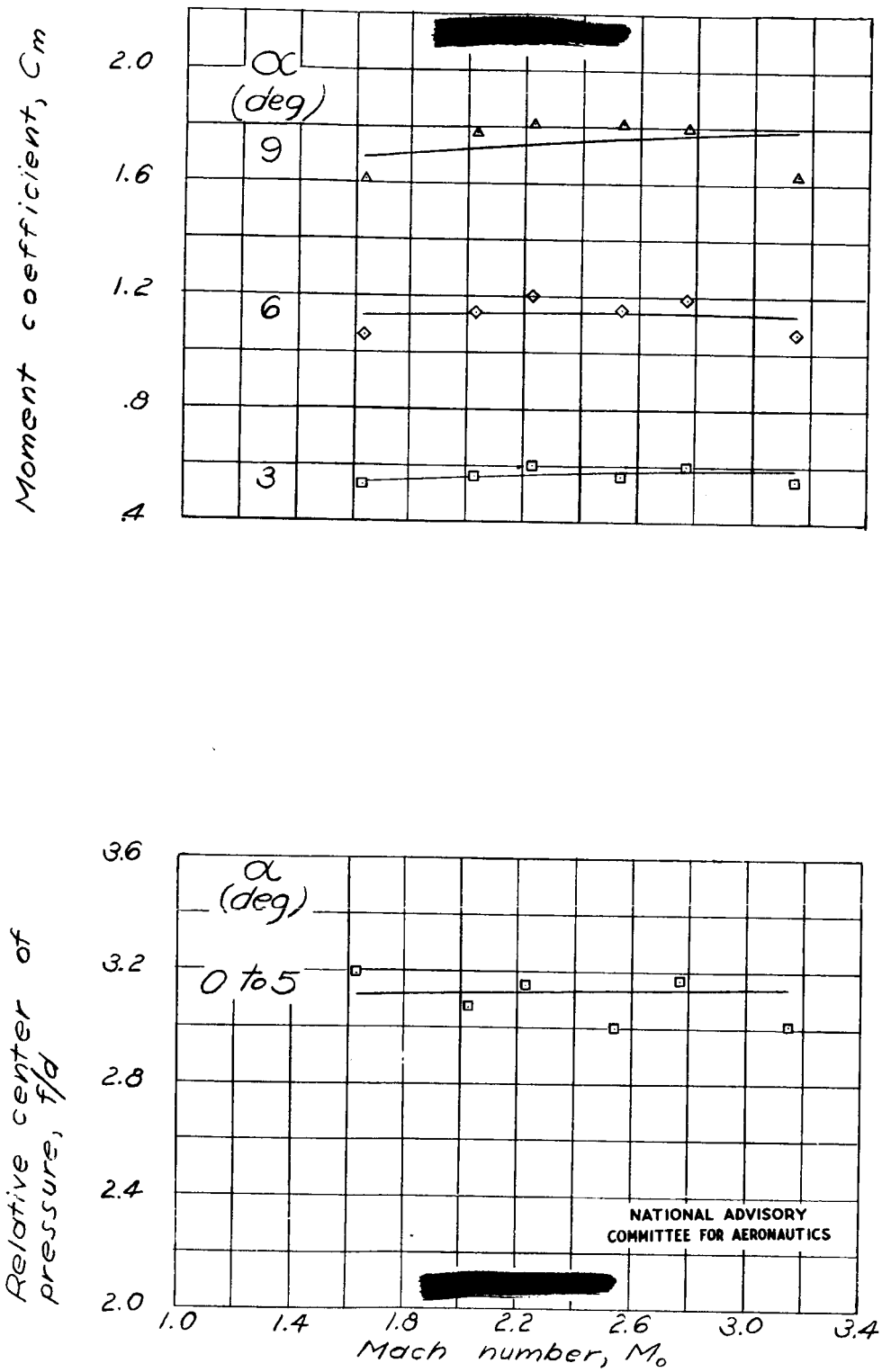

Figure 6.- Concluded.

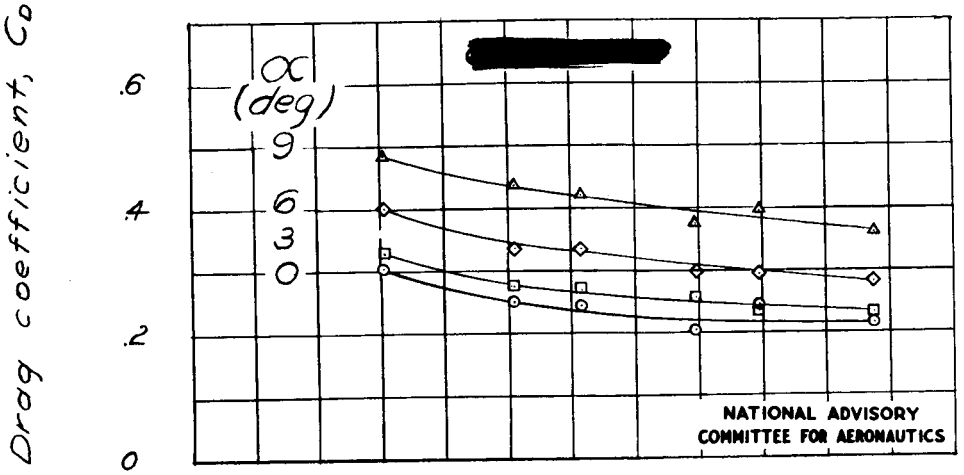

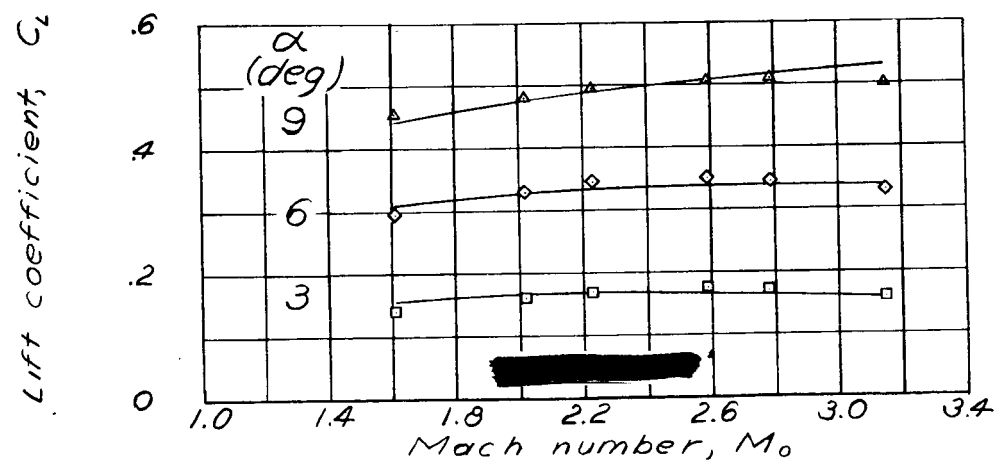

Figure 7.- Lift, drag, and moment coefficients and position of center of pressure as functions of Mach number for various angles of attack. Model 2. (Göttingen).

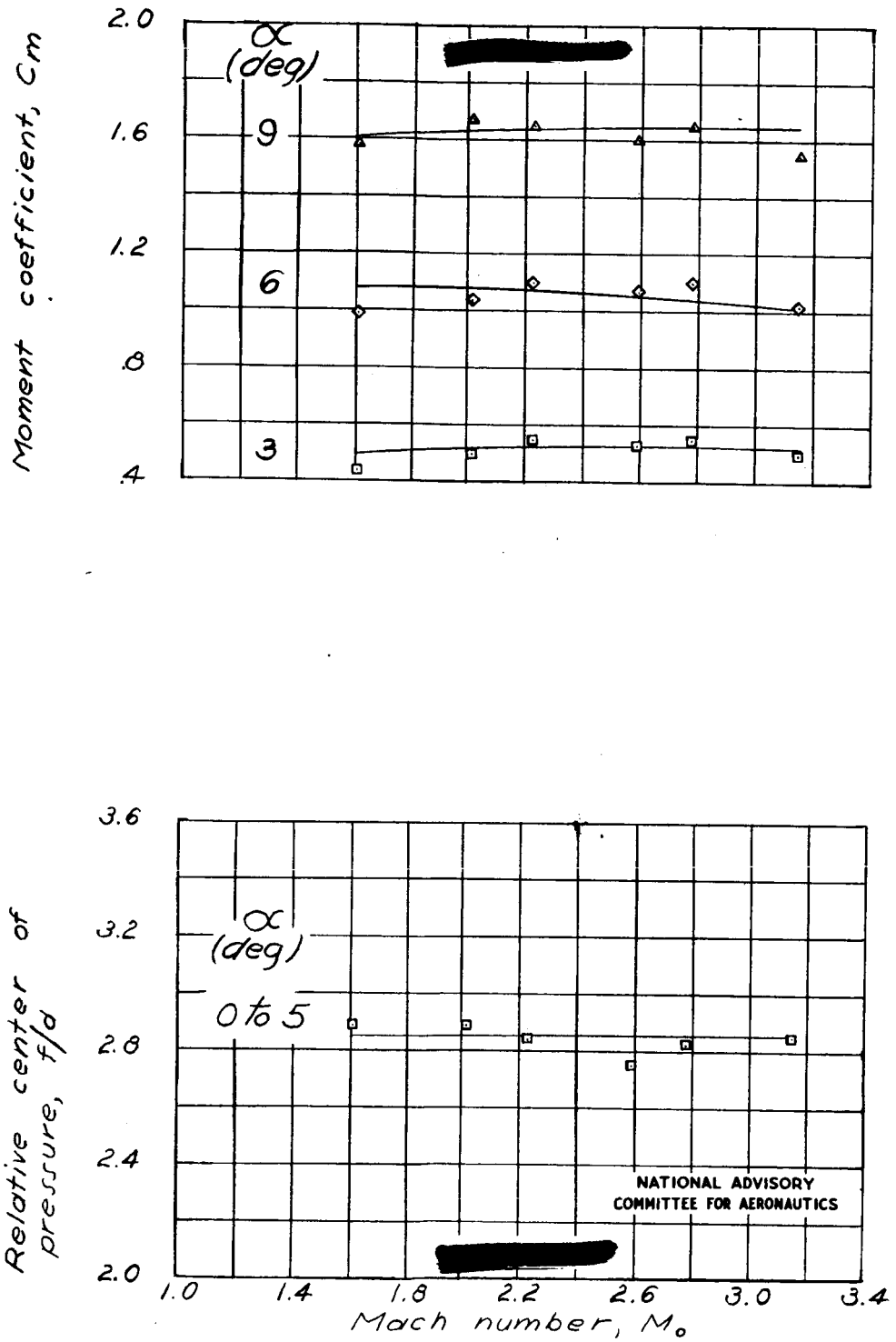

Figure 7.- Concluded.

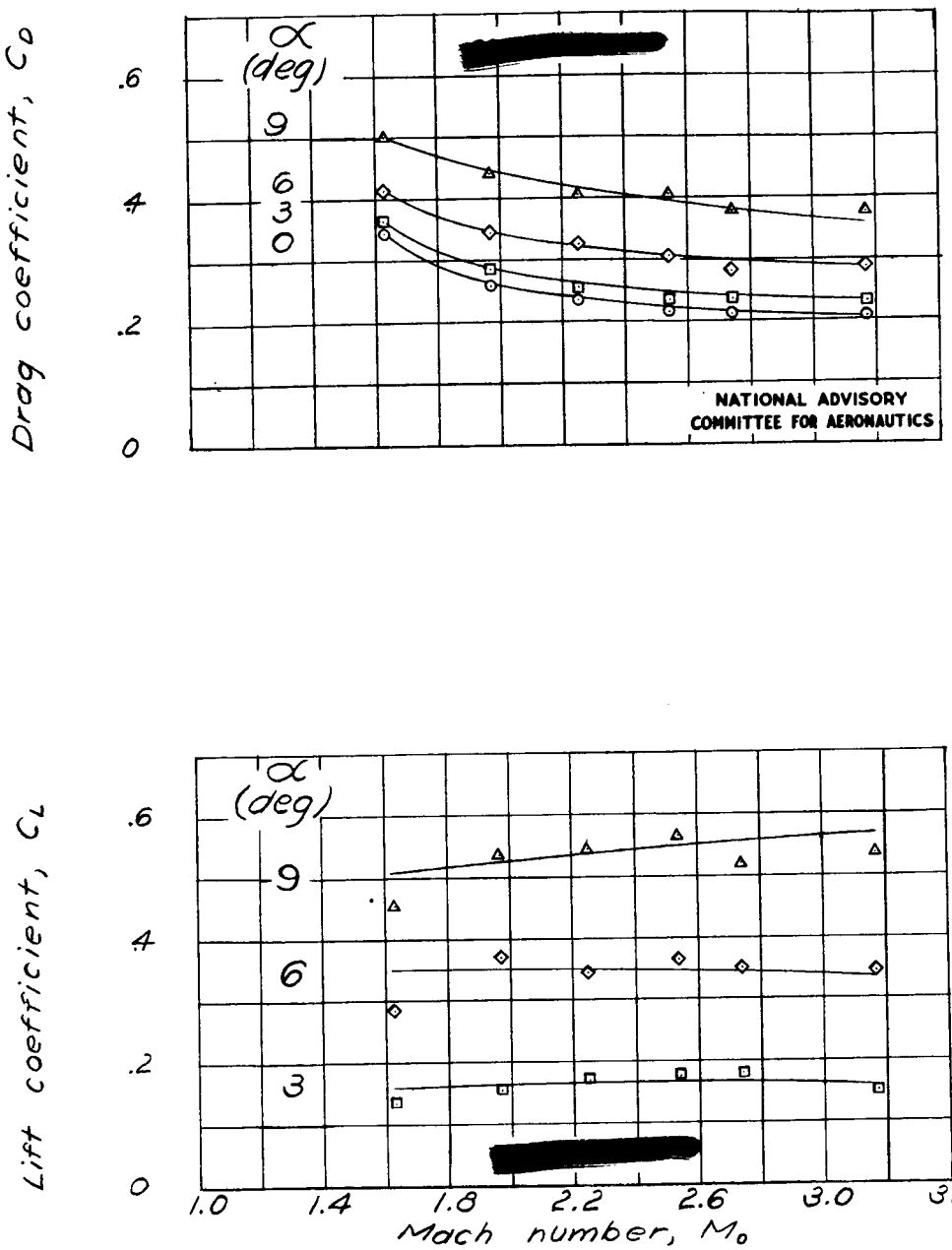

Figure 8.- Lift, drag, and moment coefficients and position of center of pressure as functions of Mach number for various angles of attack. Model 3. (Göttingen)

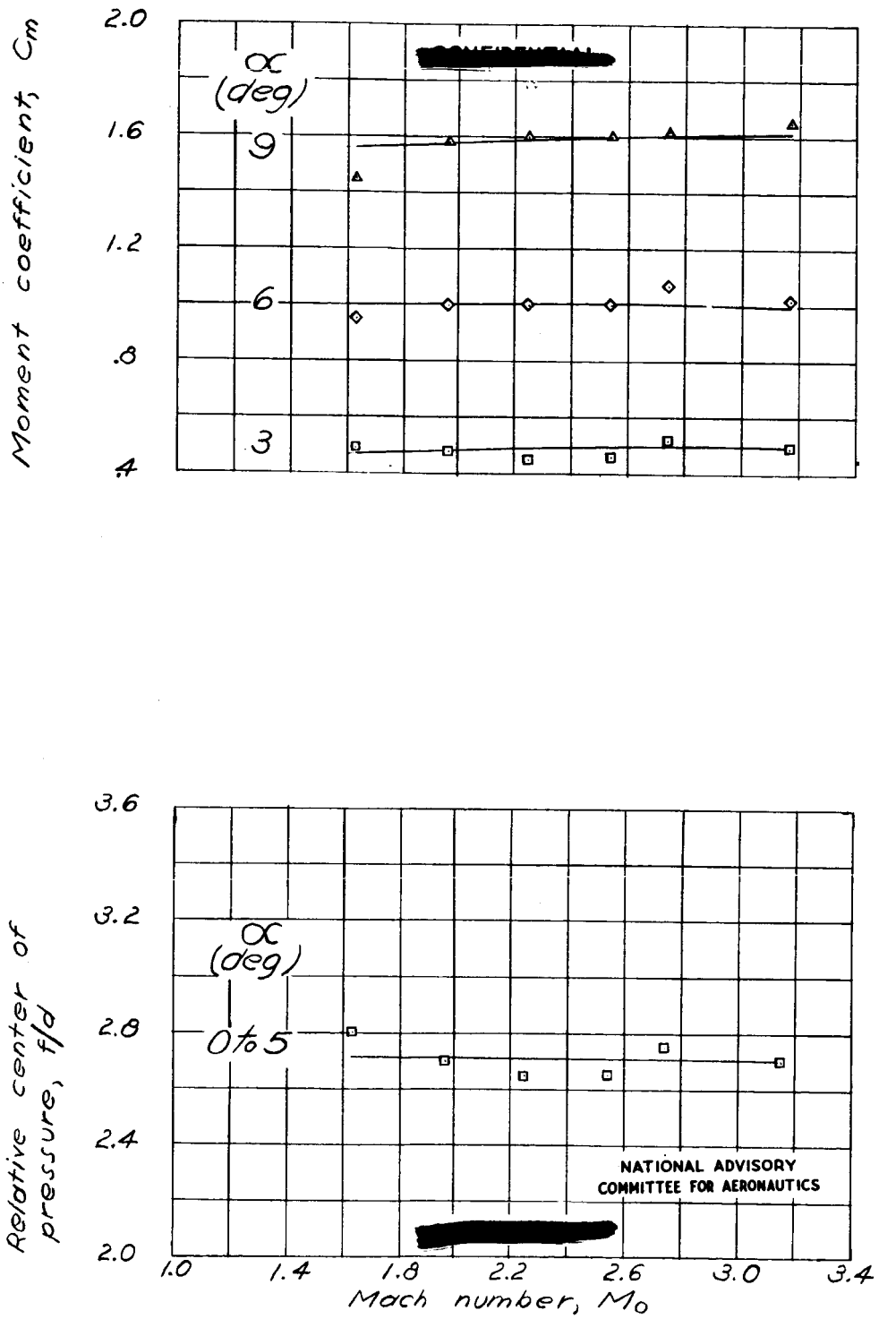

Figure 8.- Concluded.

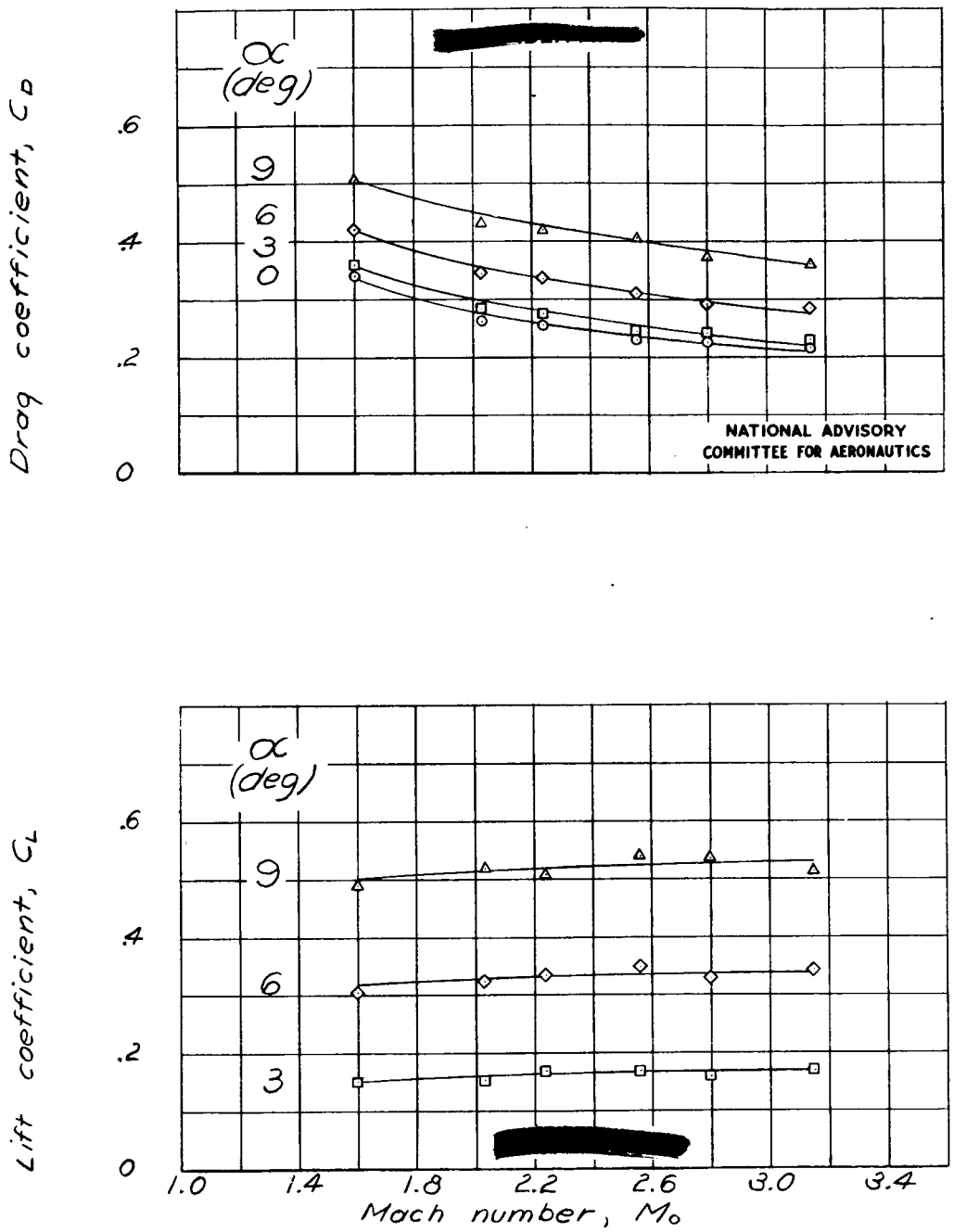

Figure 9.- Lift, drag, and moment coefficients and position of center of pressure as functions of Mach number for various angles of attack. Model 4. (Göttingen)

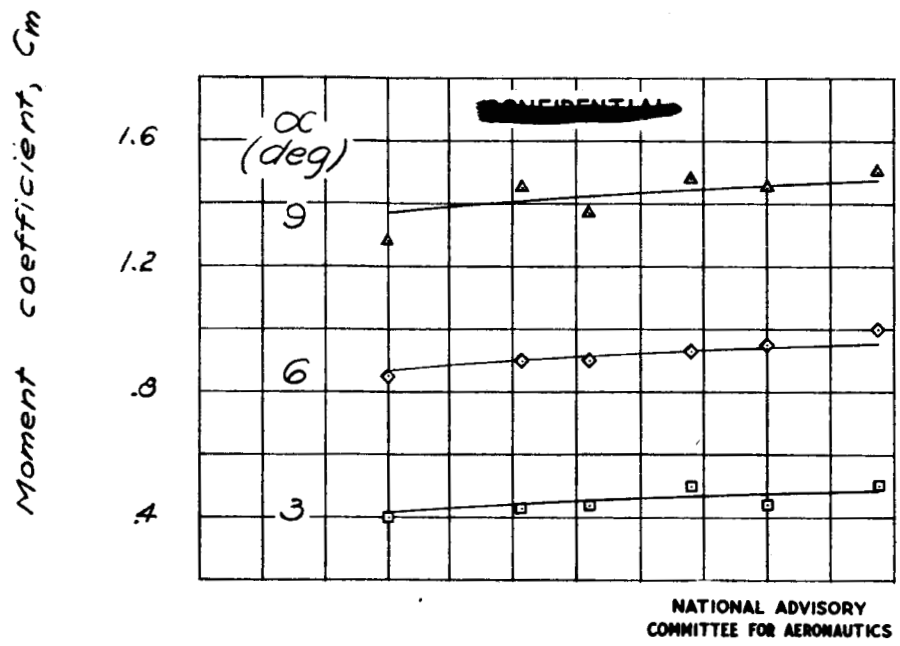

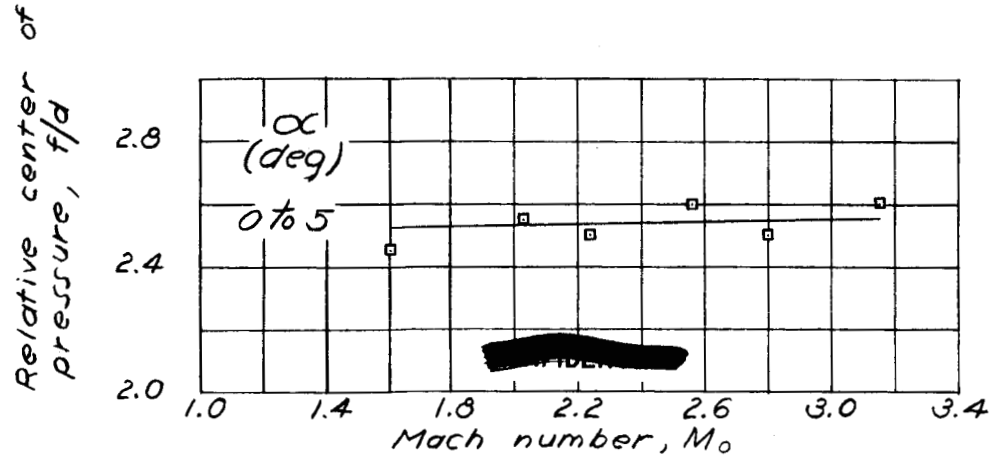

Figure 9.- Concluded.

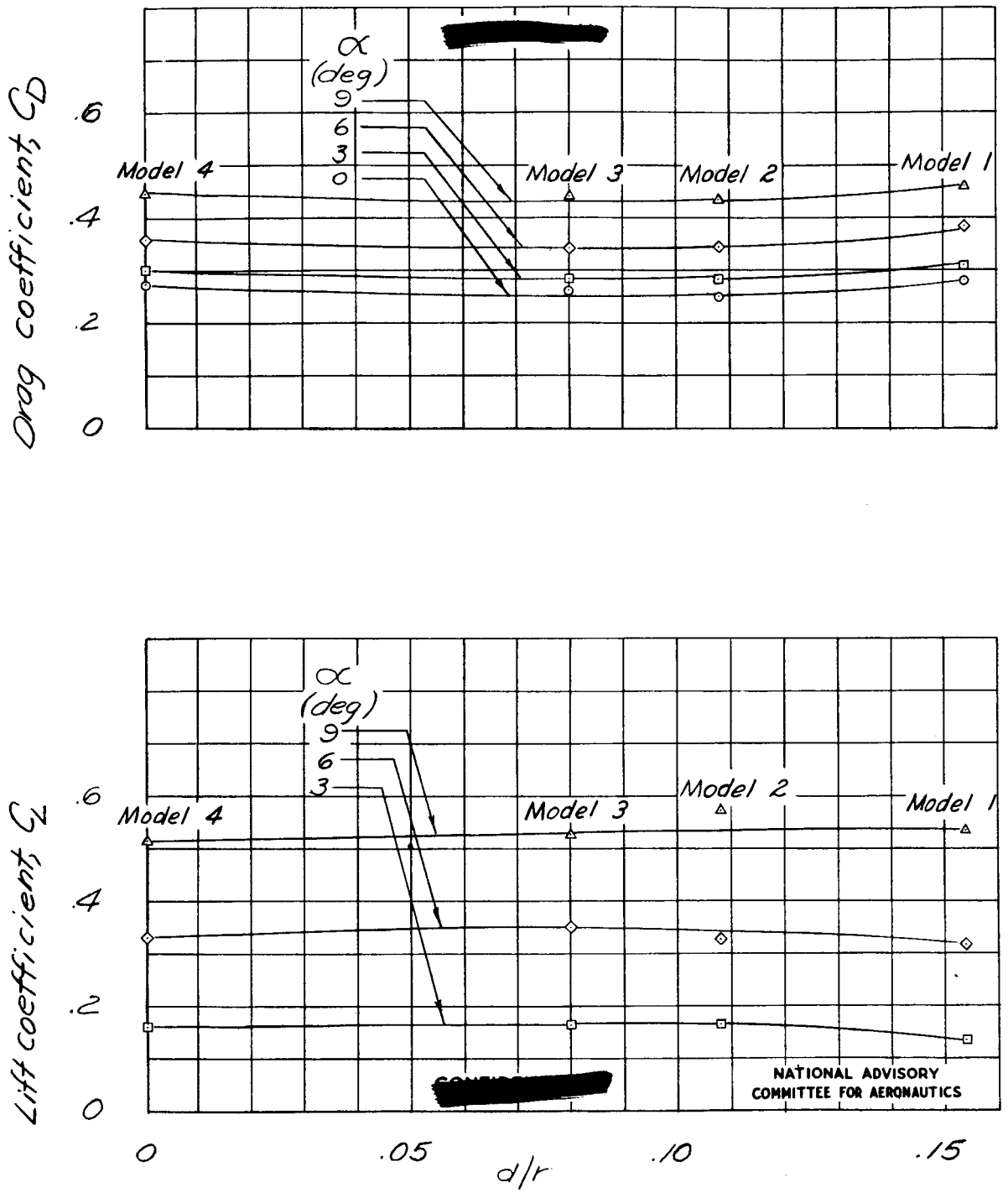

Figure 10.- Lift, drag, and moment coefficients and position of center of pressure as functions of the ratio of the diameter of the body of the projectile to the radius of the nose of the projectile for various angles of attack. M_o = 2.0. (Göttingen)

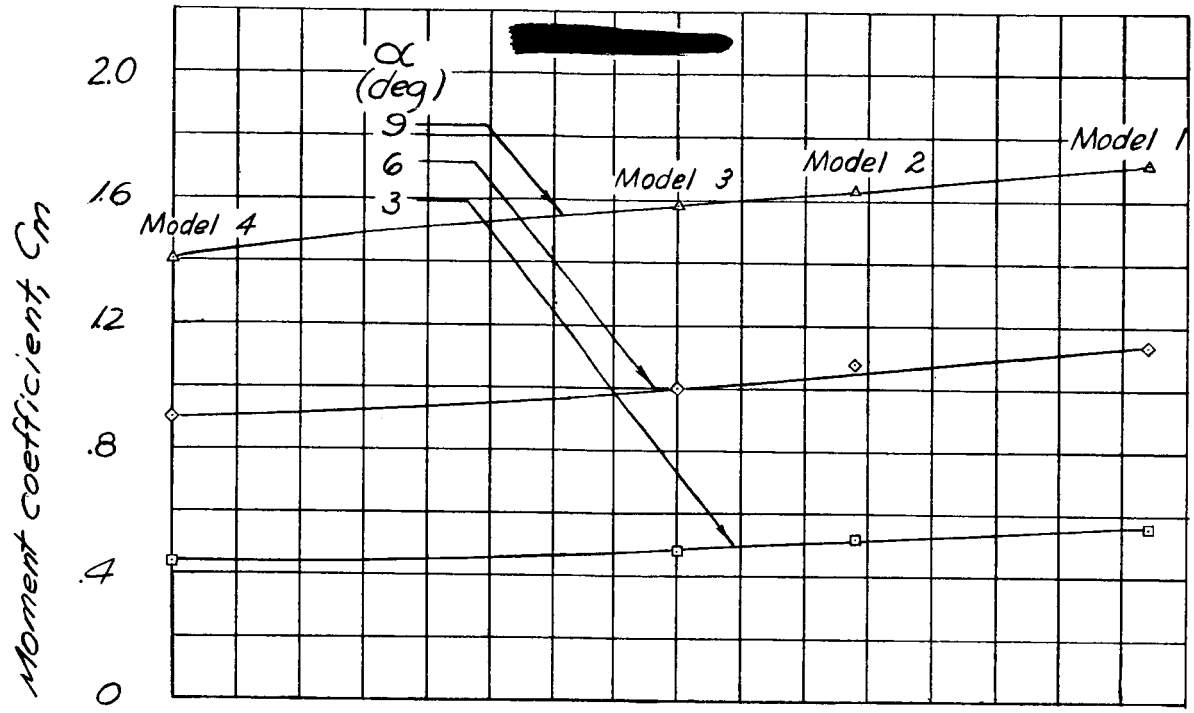

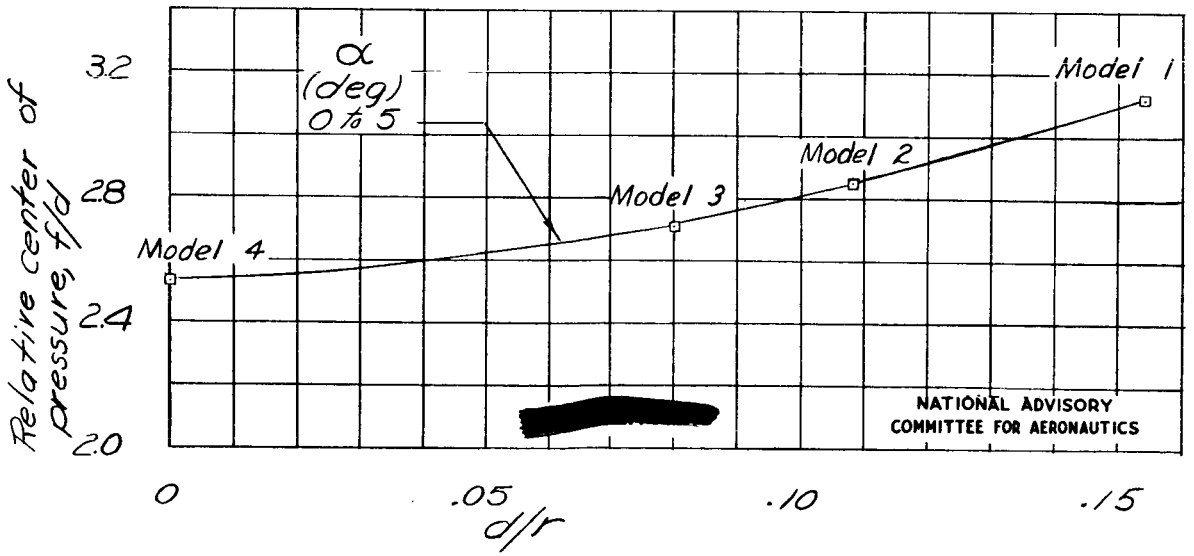

Figure 10.- Concluded.

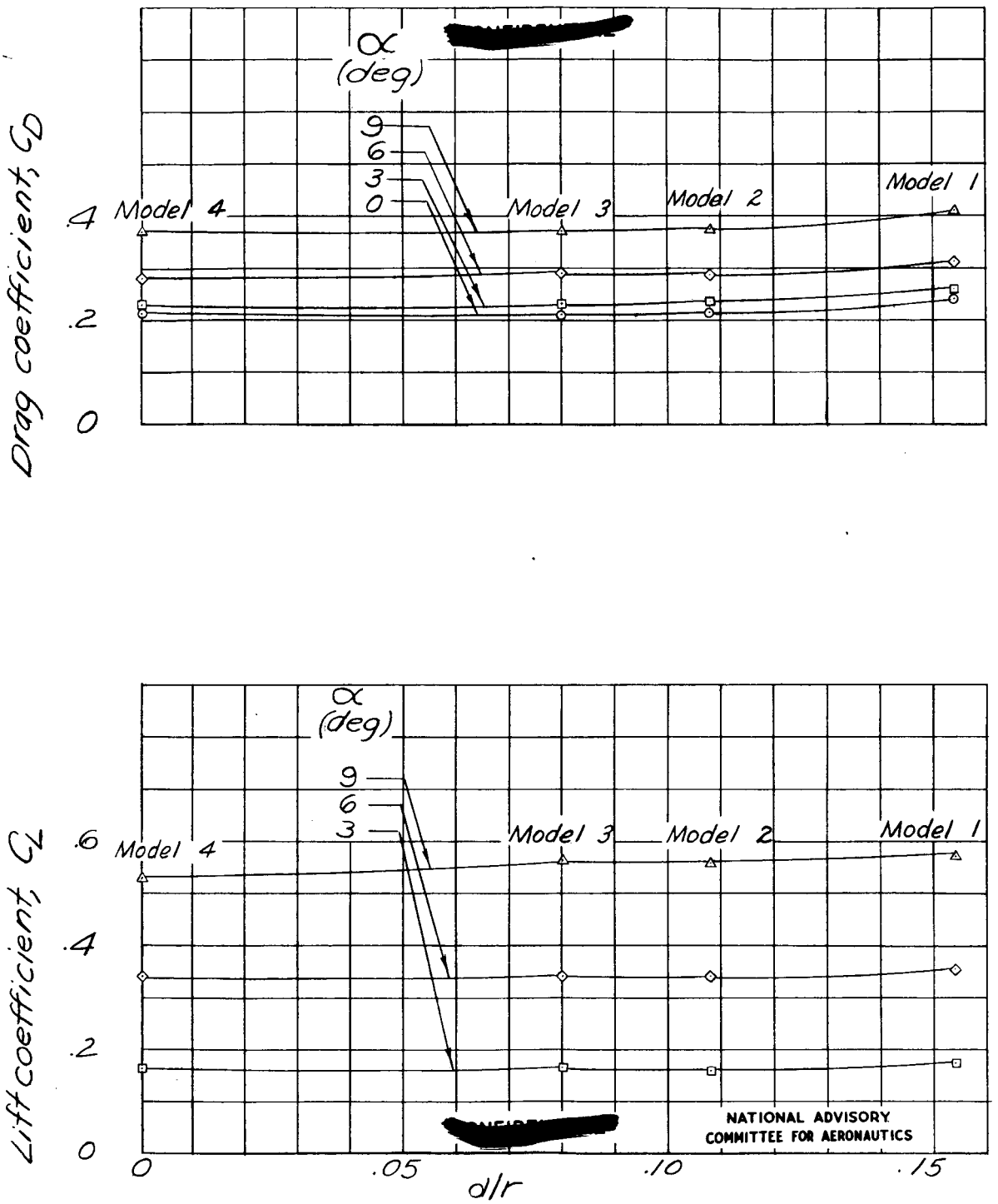

Figure 11.- Lift, drag, and moment coefficients and position of center of pressure as functions of the ratio of the diameter of the body of the projectile to the radius of the nose of the projectile for various angles of attack. M_o = 3.0. (Göttingen)

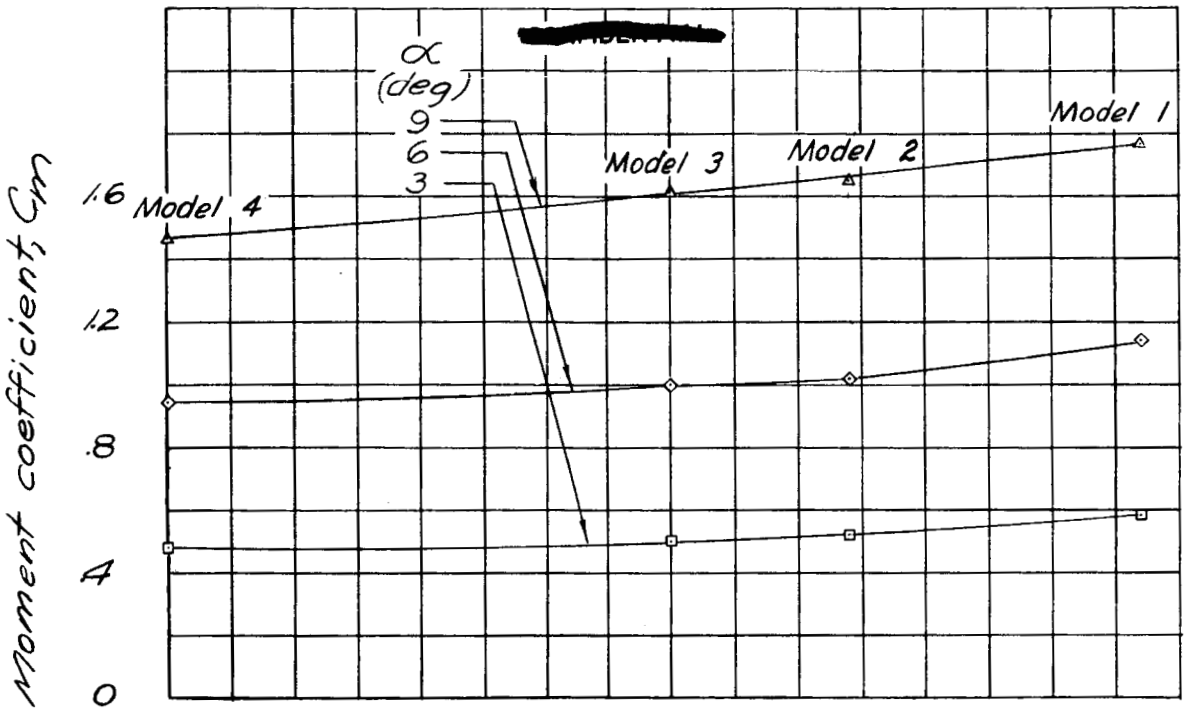

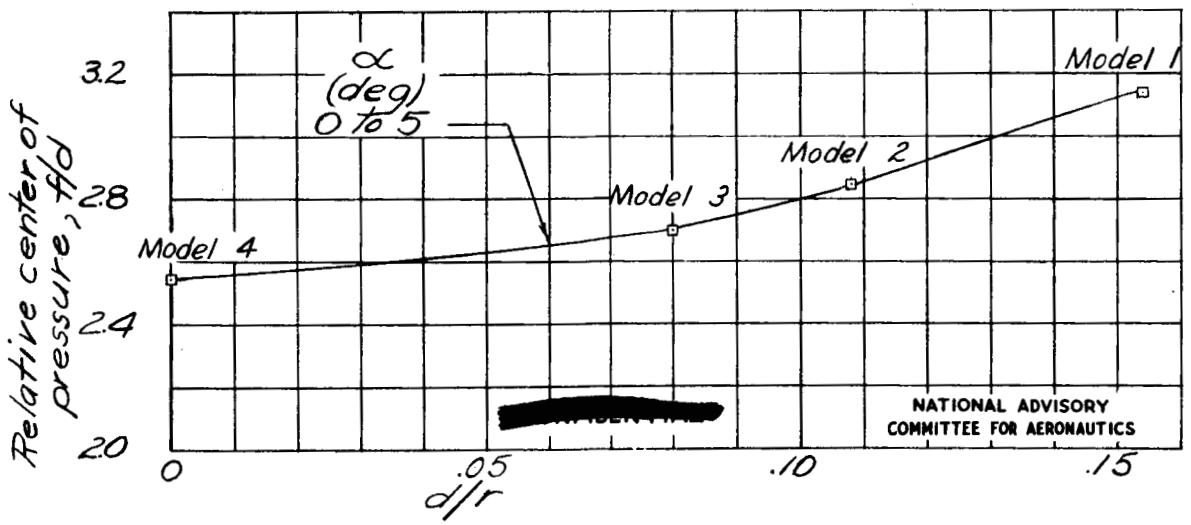

Figure 11.- Concluded.

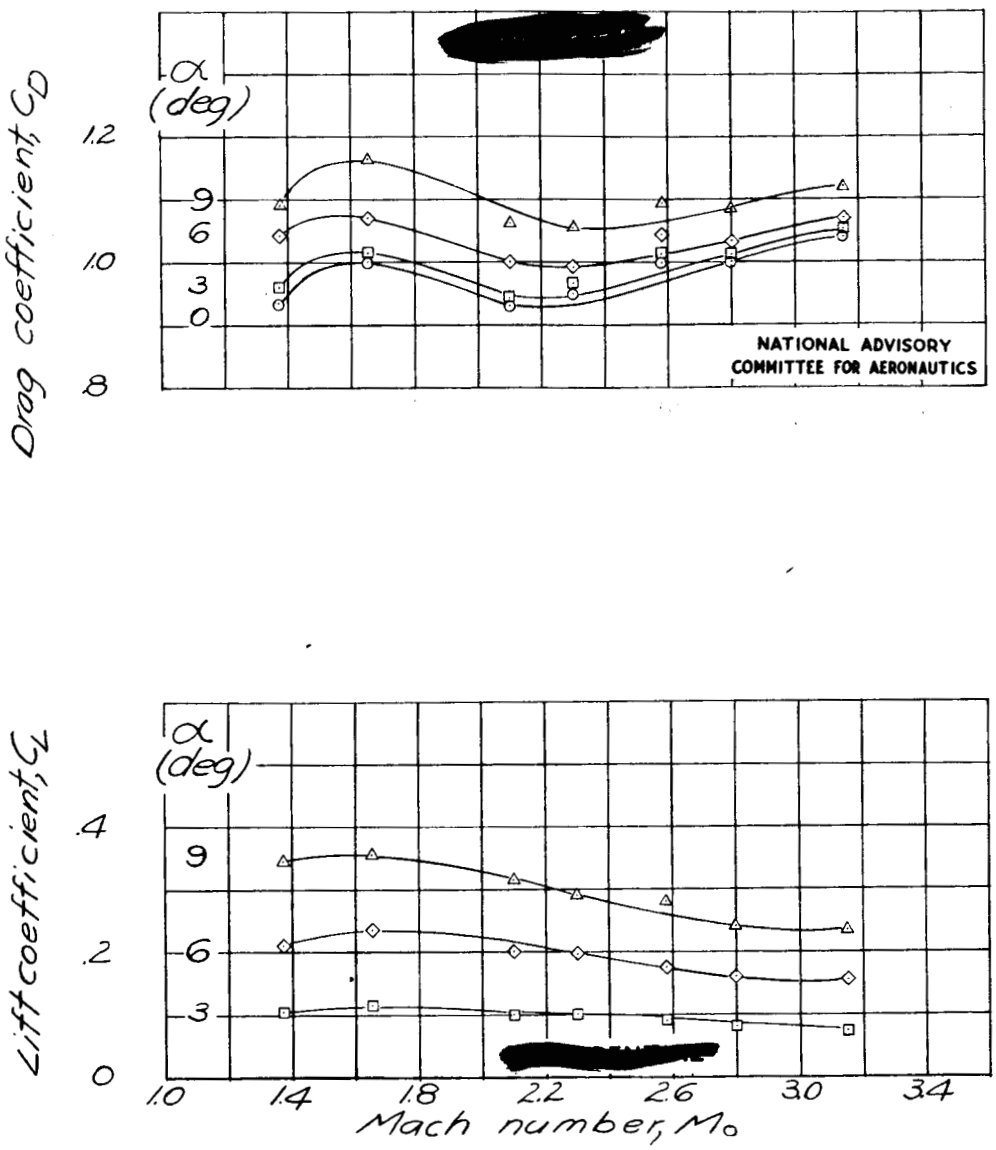

Figure 12.- Lift, drag, and moment coefficients and position of center of pressure as functions of Mach number for various angles of attack. Model 5. (Göttingen)

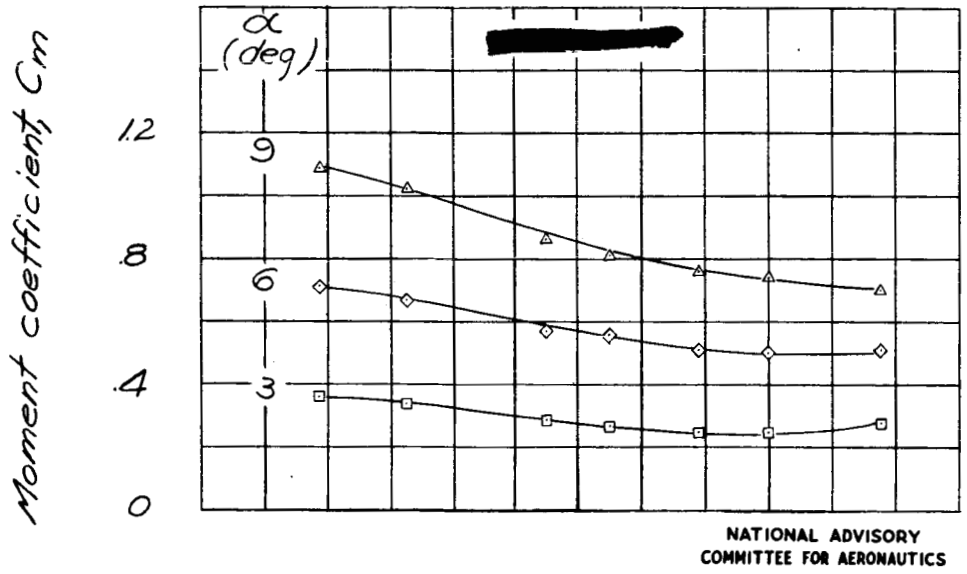

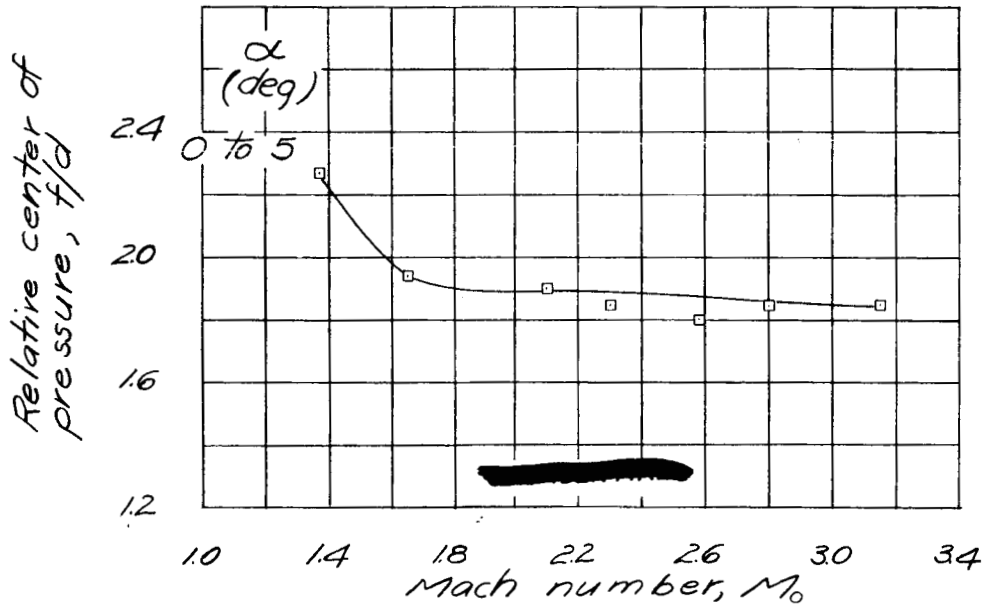

Figure 12.- Concluded.

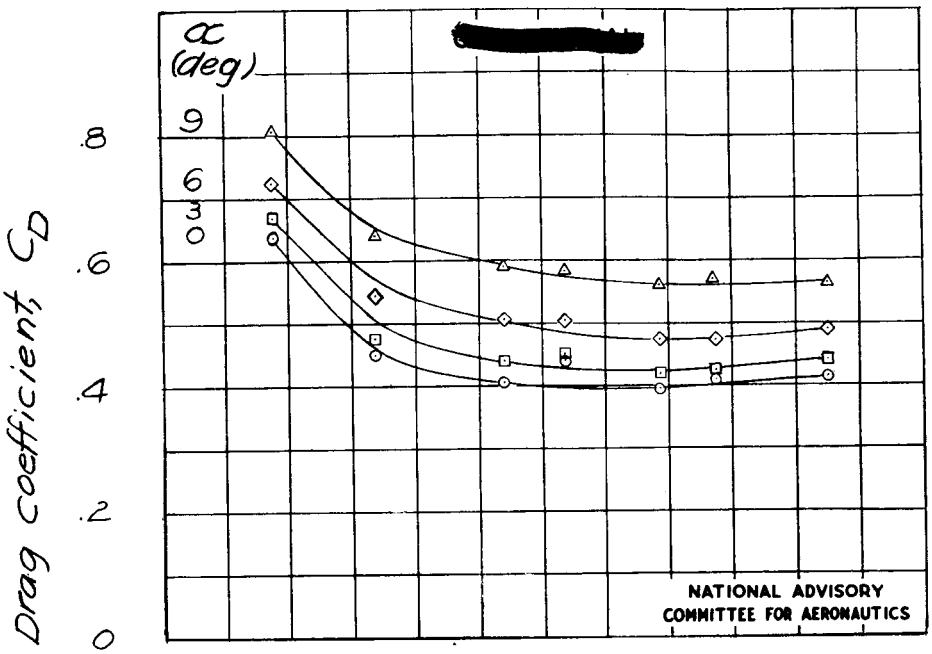

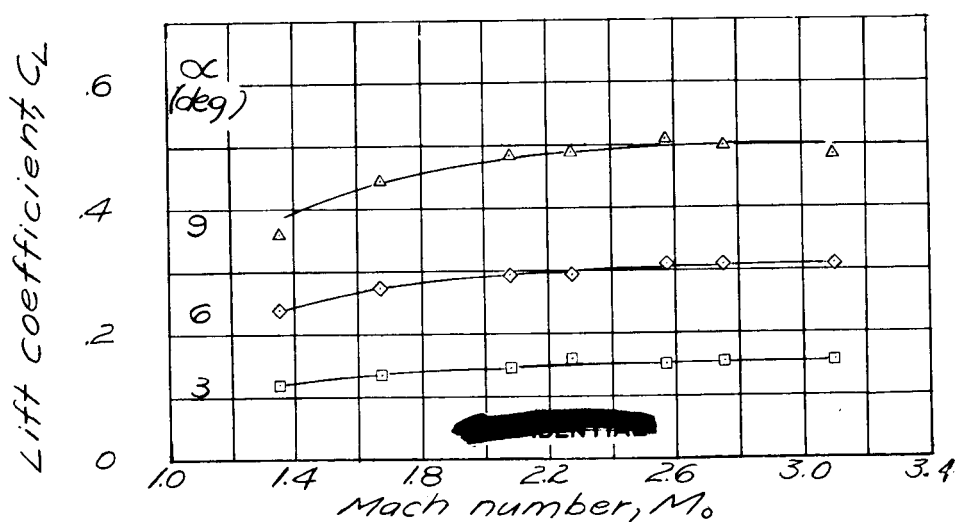

Figure 13.- Lift, drag, and moment coefficients and position of center of pressure as functions of Mach number for various angles of attack. Model 6. (Göttingen)

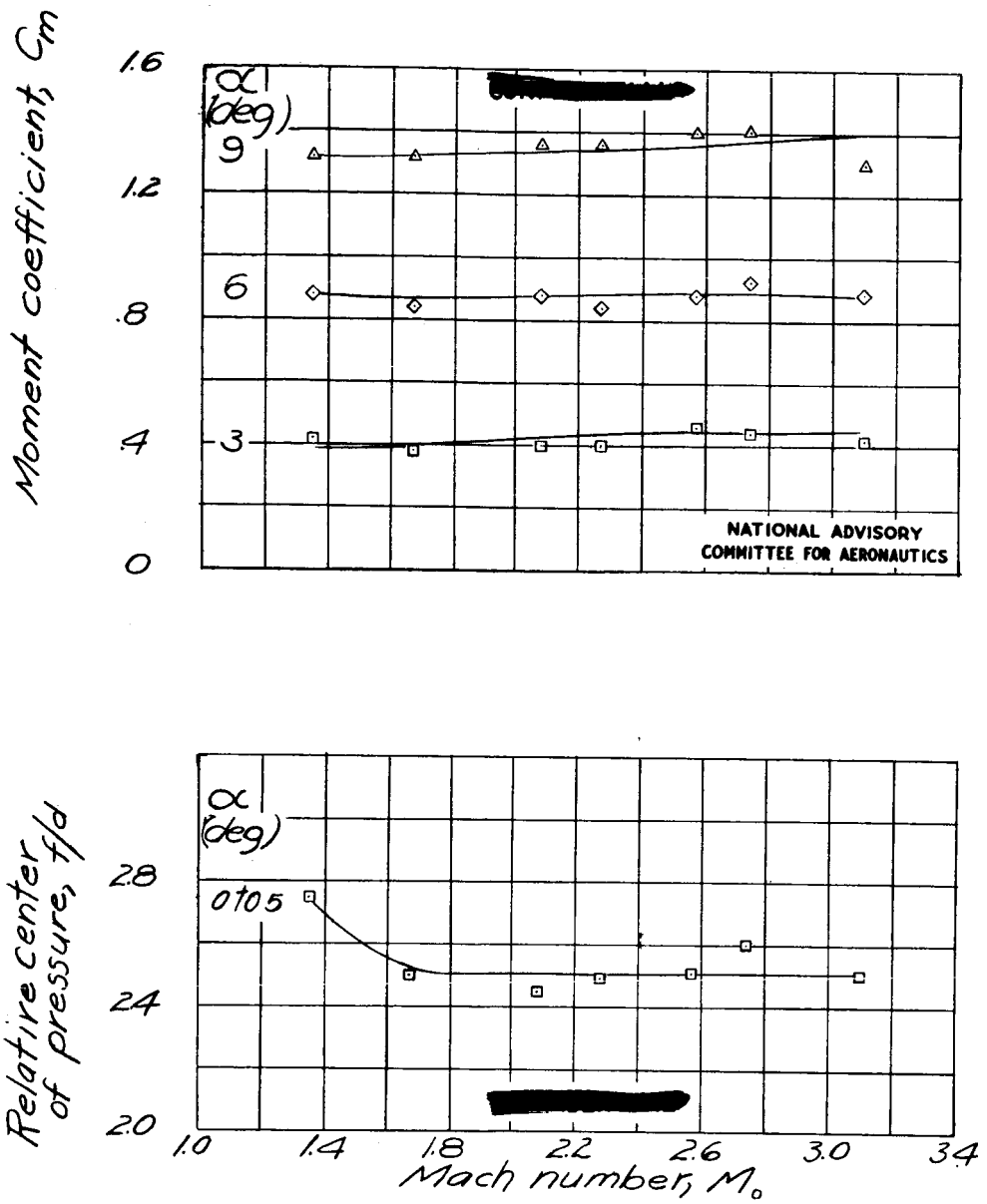

Figure 13.- Concluded.

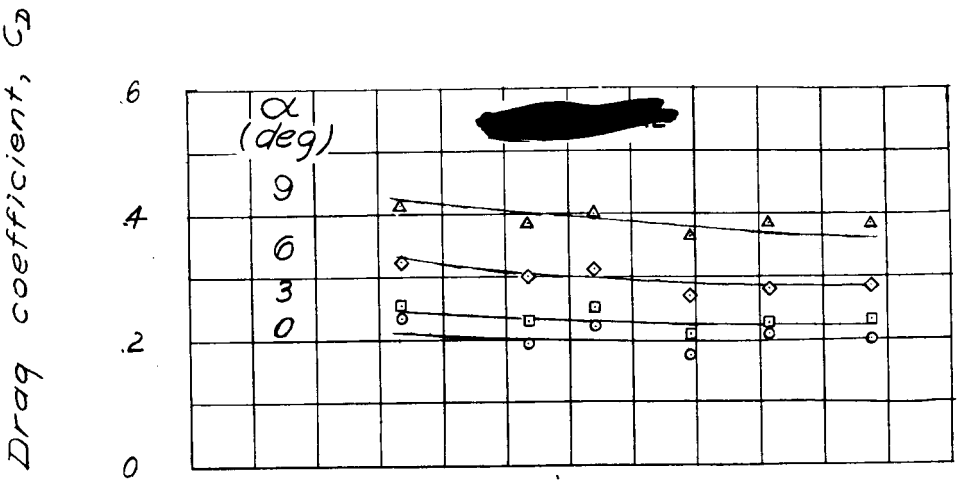

NATIONAL ADVISORY
COMMITTEE FOR AERONAUTICS

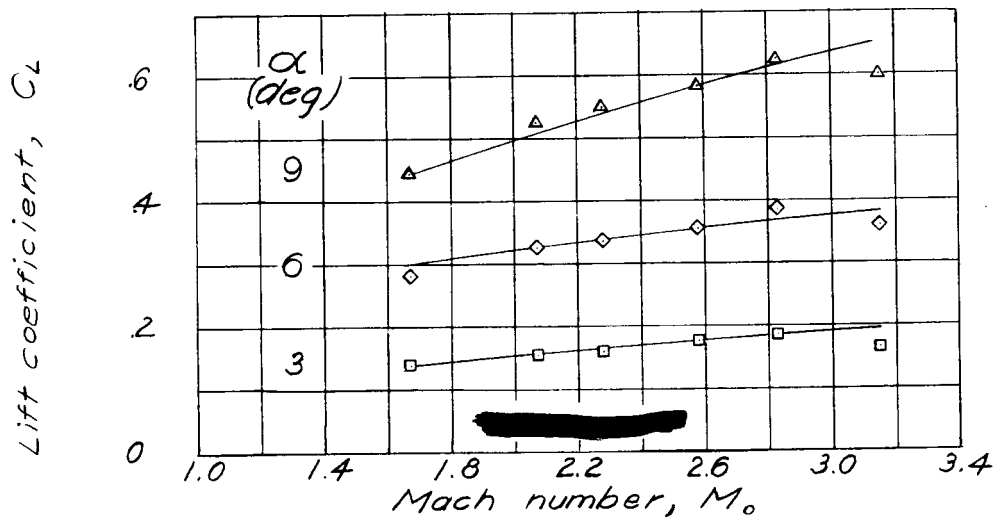

Figure 14. - Lift, drag, and moment coefficients and position of center of pressure as functions of Mach number for various angles of attack. Model 7. (Göttingen)

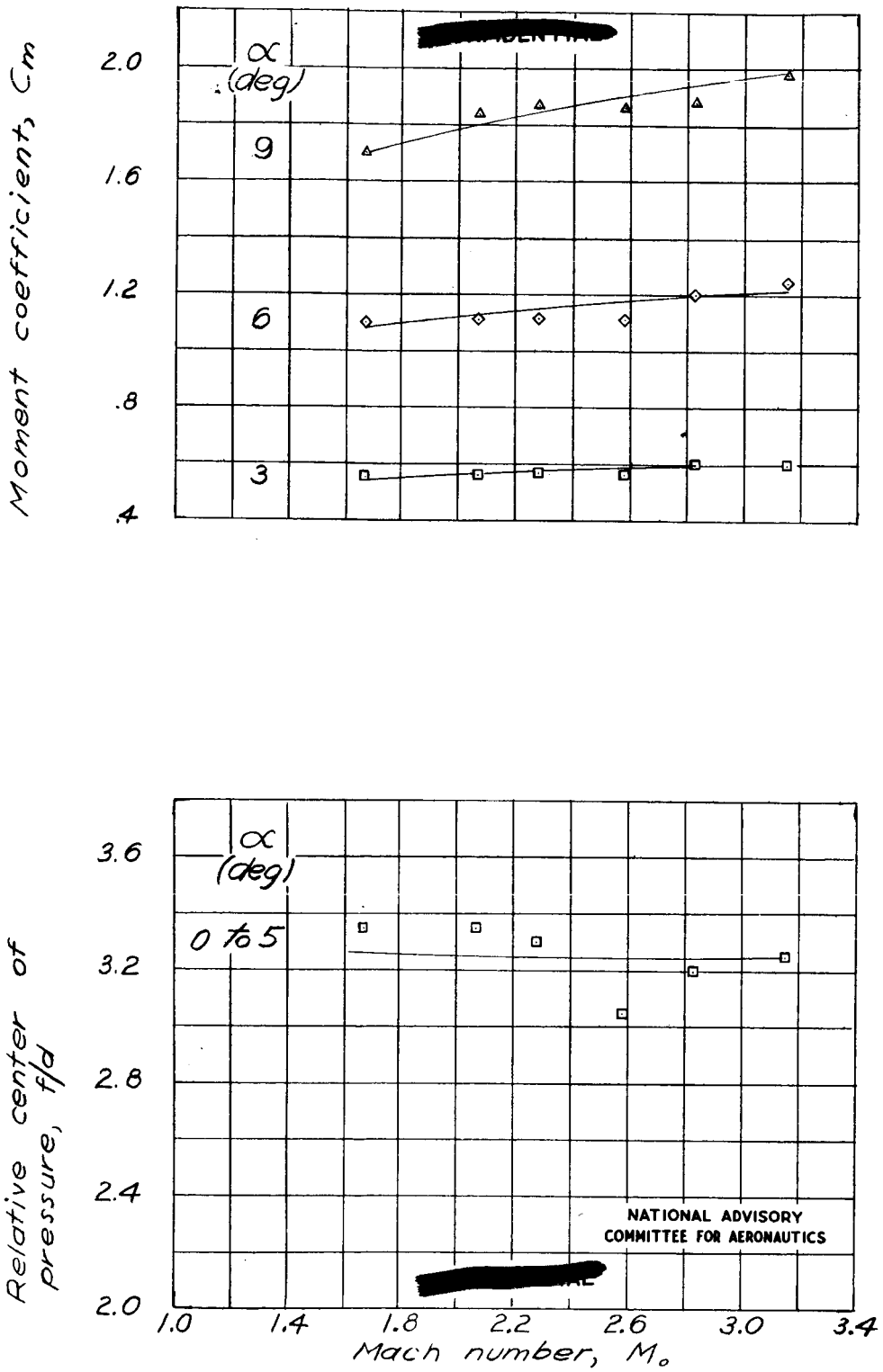

Figure 14.- Concluded.

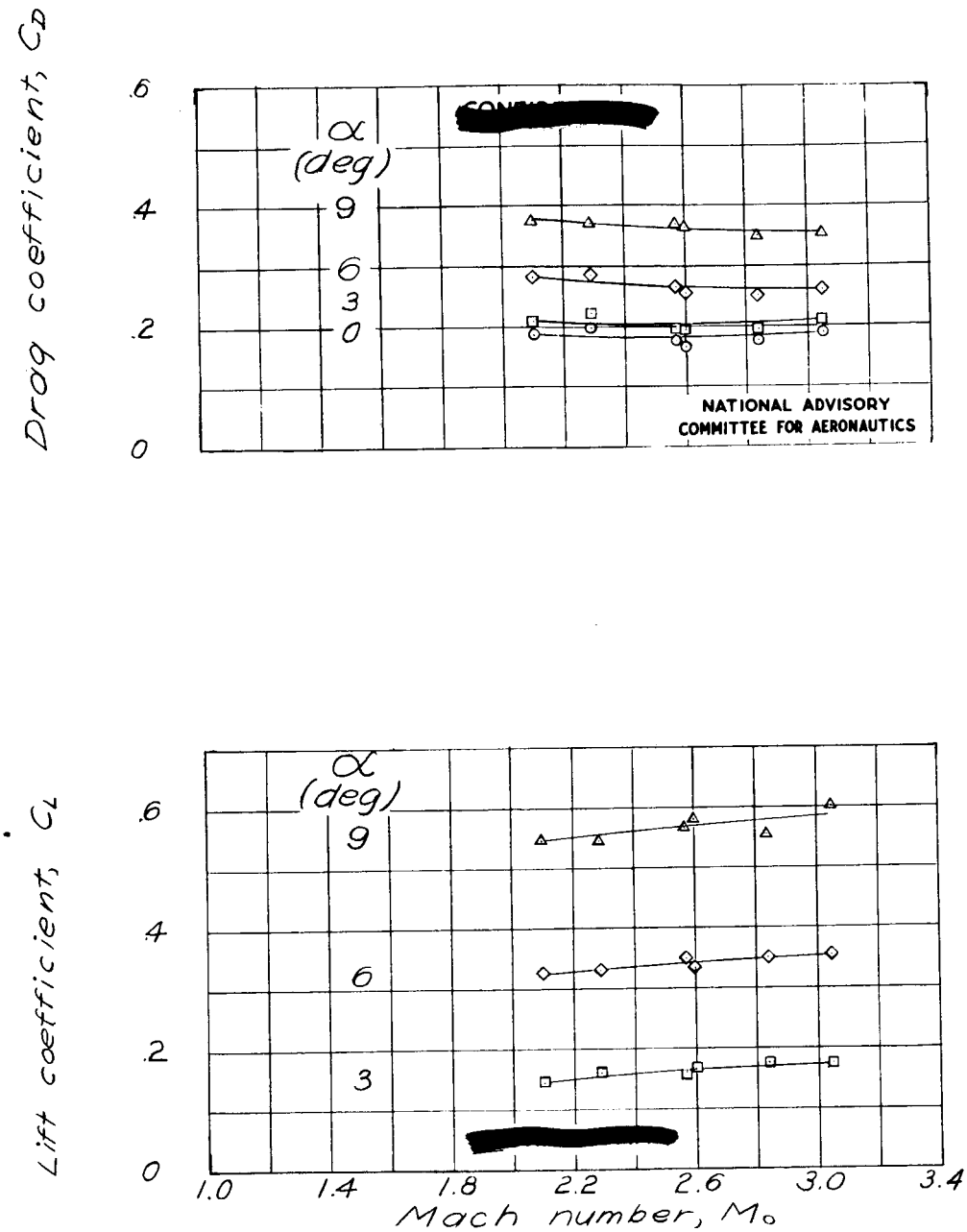

Figure 15.- Lift, drag, and moment coefficients and position of center of pressure as functions of Mach number for various angles of attack. Model 8. (Göttingen)

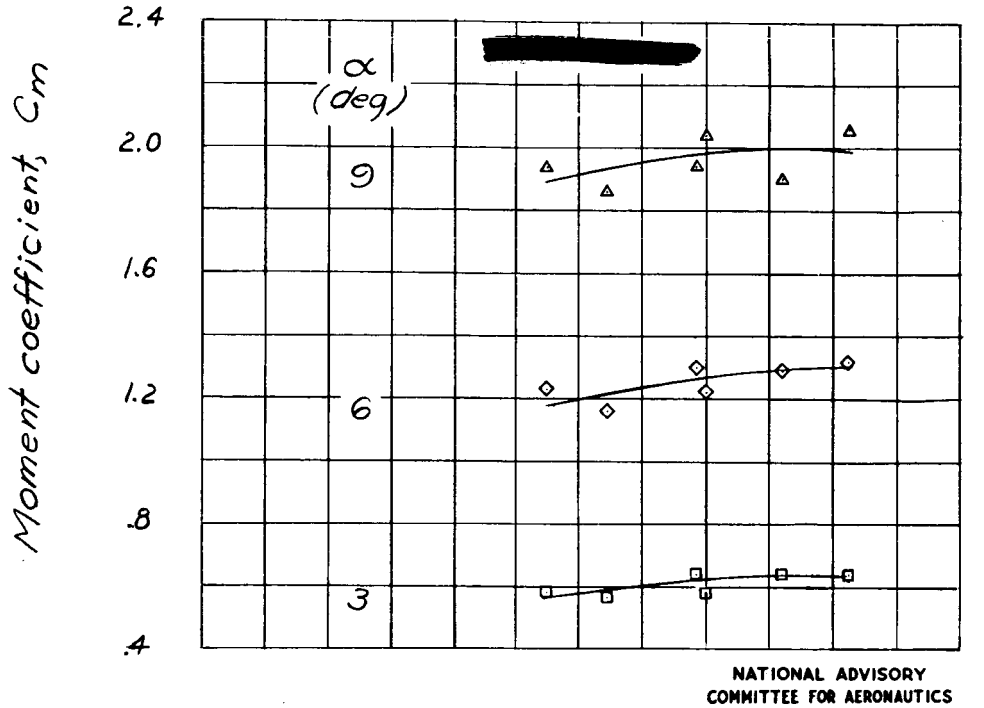

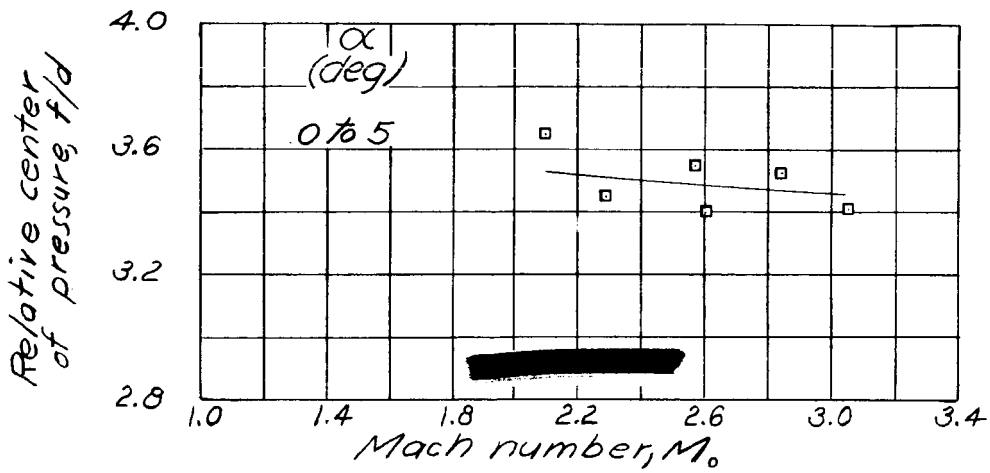

Figure 15.- Concluded.

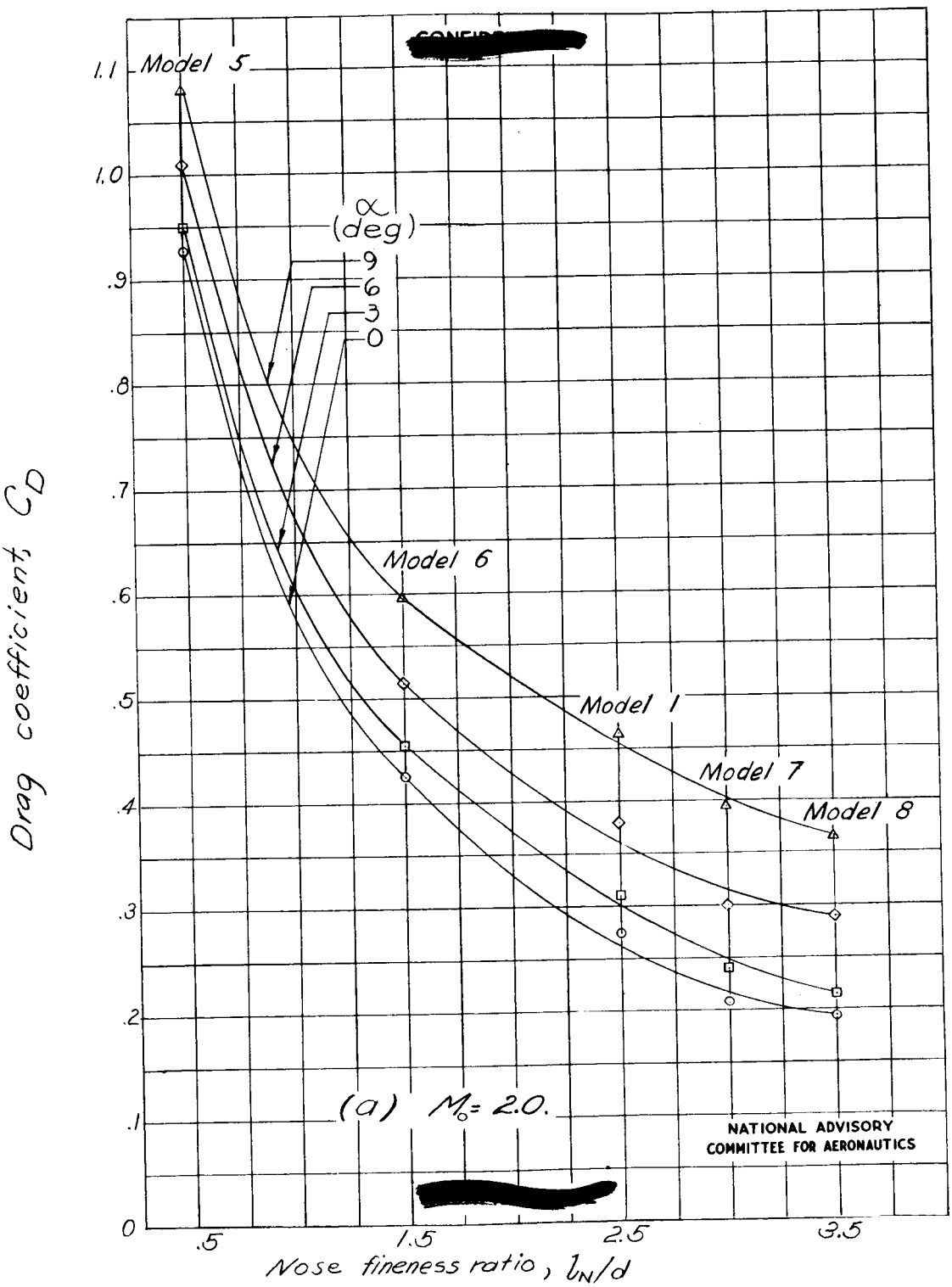

Figure 16.- Drag coefficient as a function of nose fineness ratio for constant Mach number. (Göttingen)

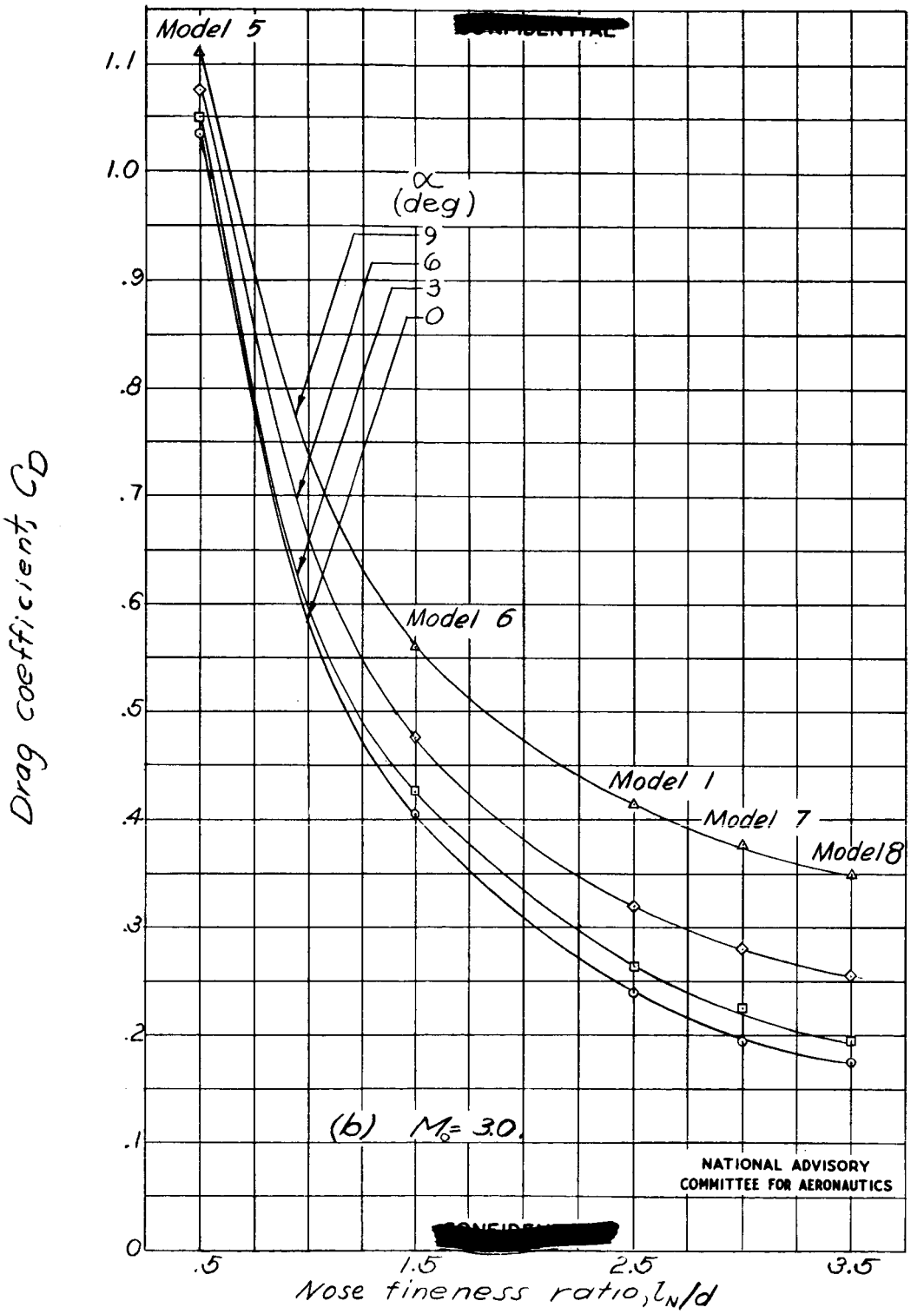

Figure 16.- Concluded.

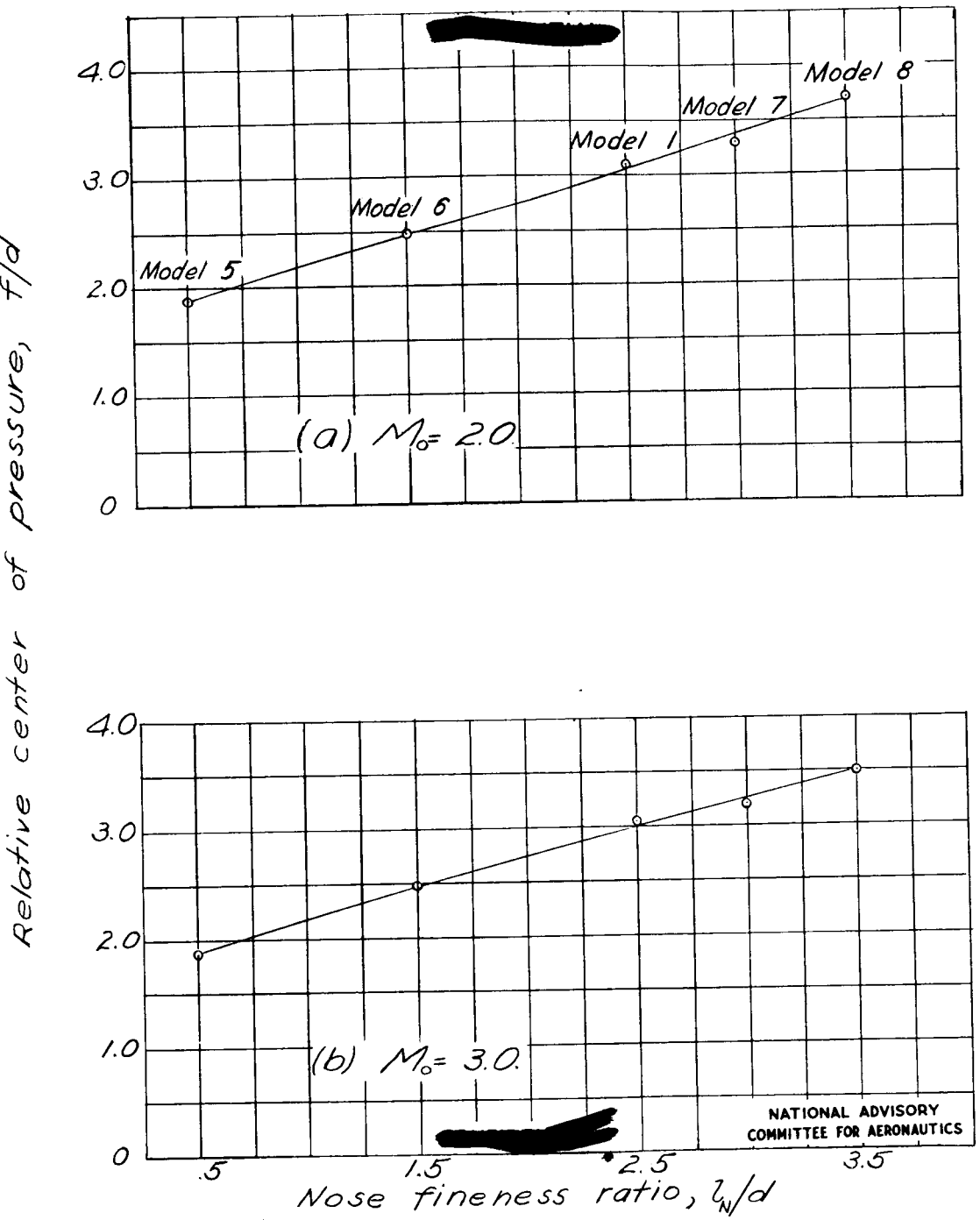

Figure 17.- Relative center of pressure as a function of nose fineness ratio for constant Mach number. (Göttingen)

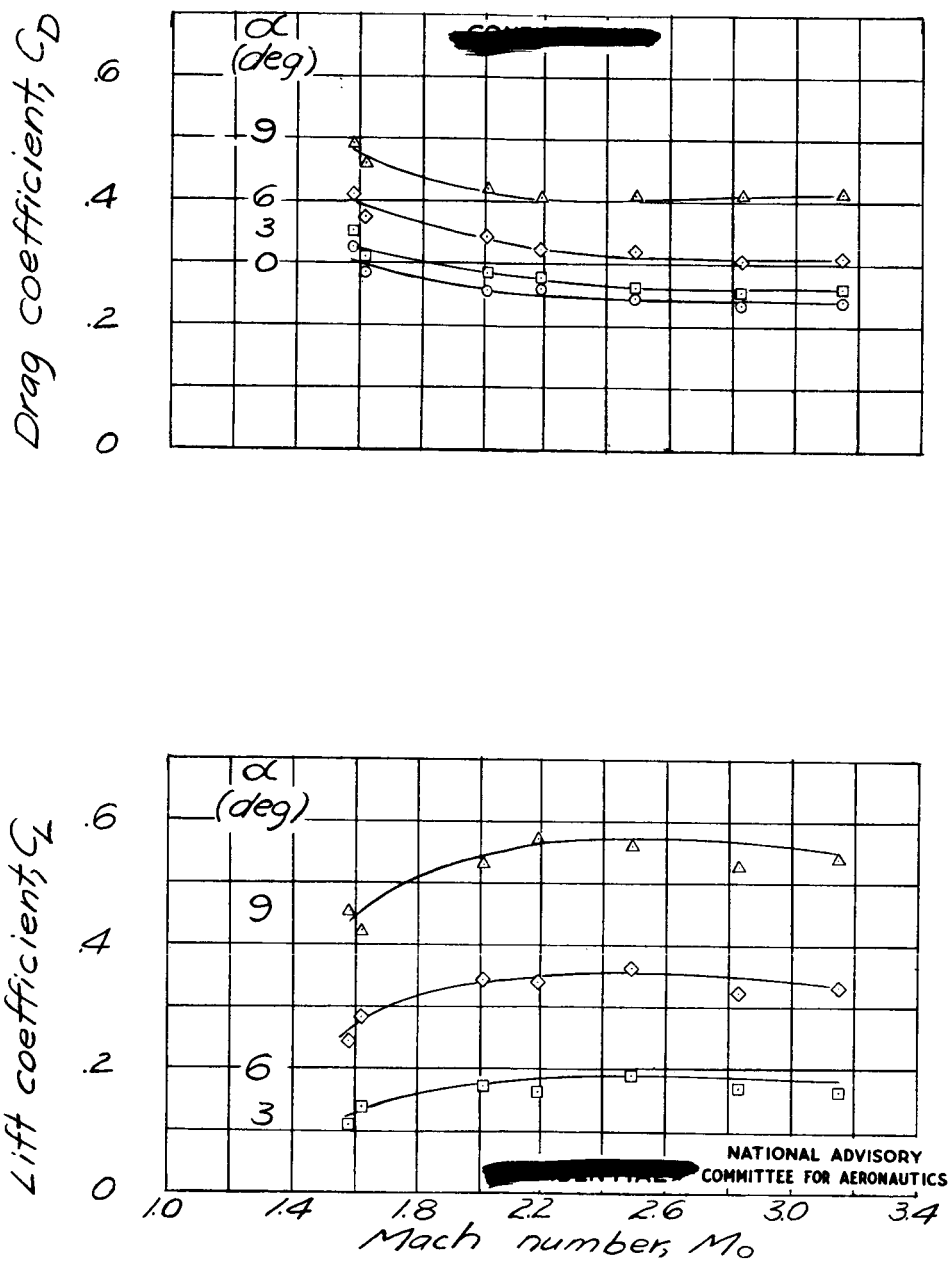

Figure 18.- Lift, drag, and moment coefficients and position of center of pressure as functions of Mach number for various angles of attack. Model 9. (Göttingen)

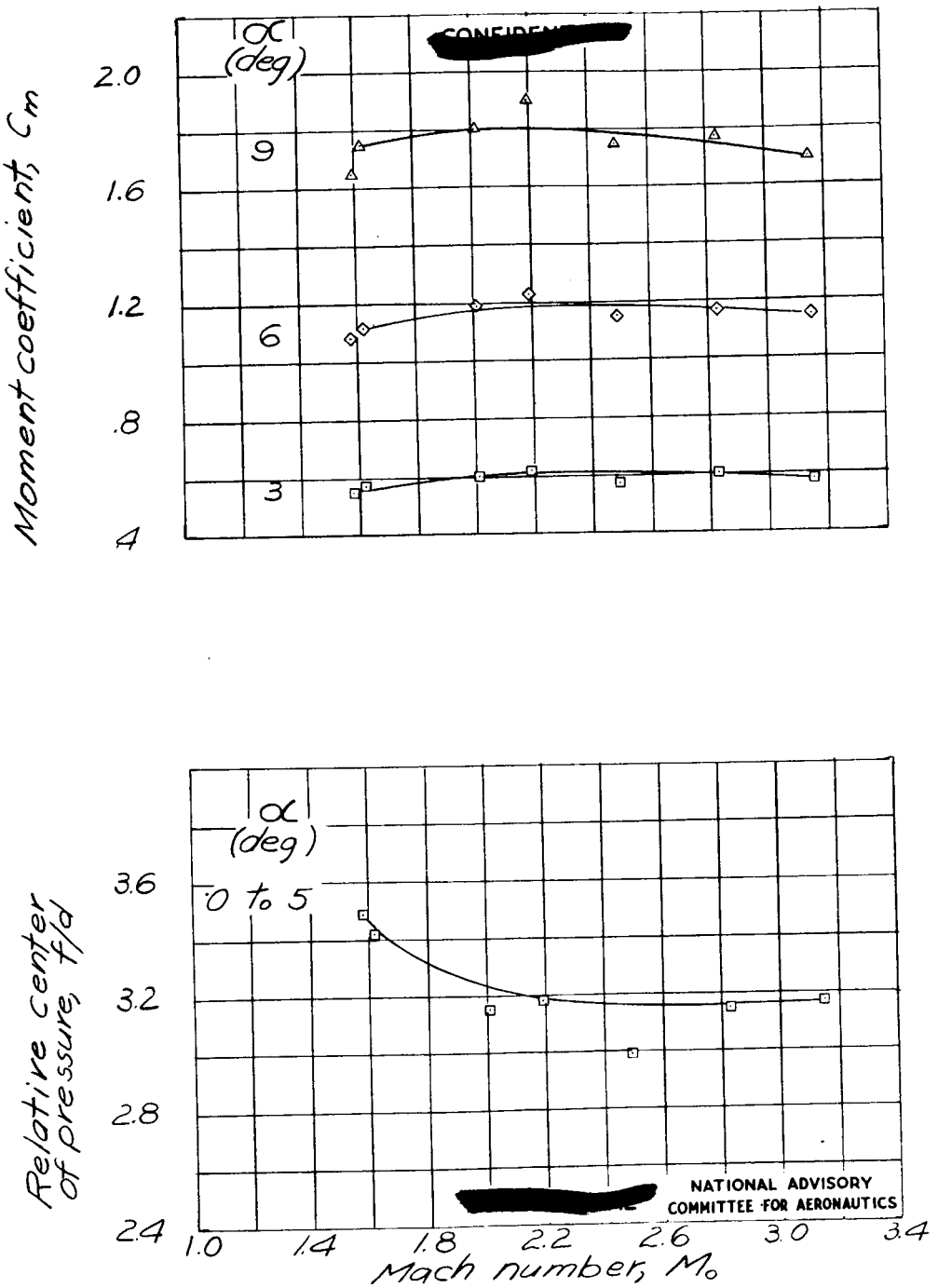

Figure 18.- Concluded.

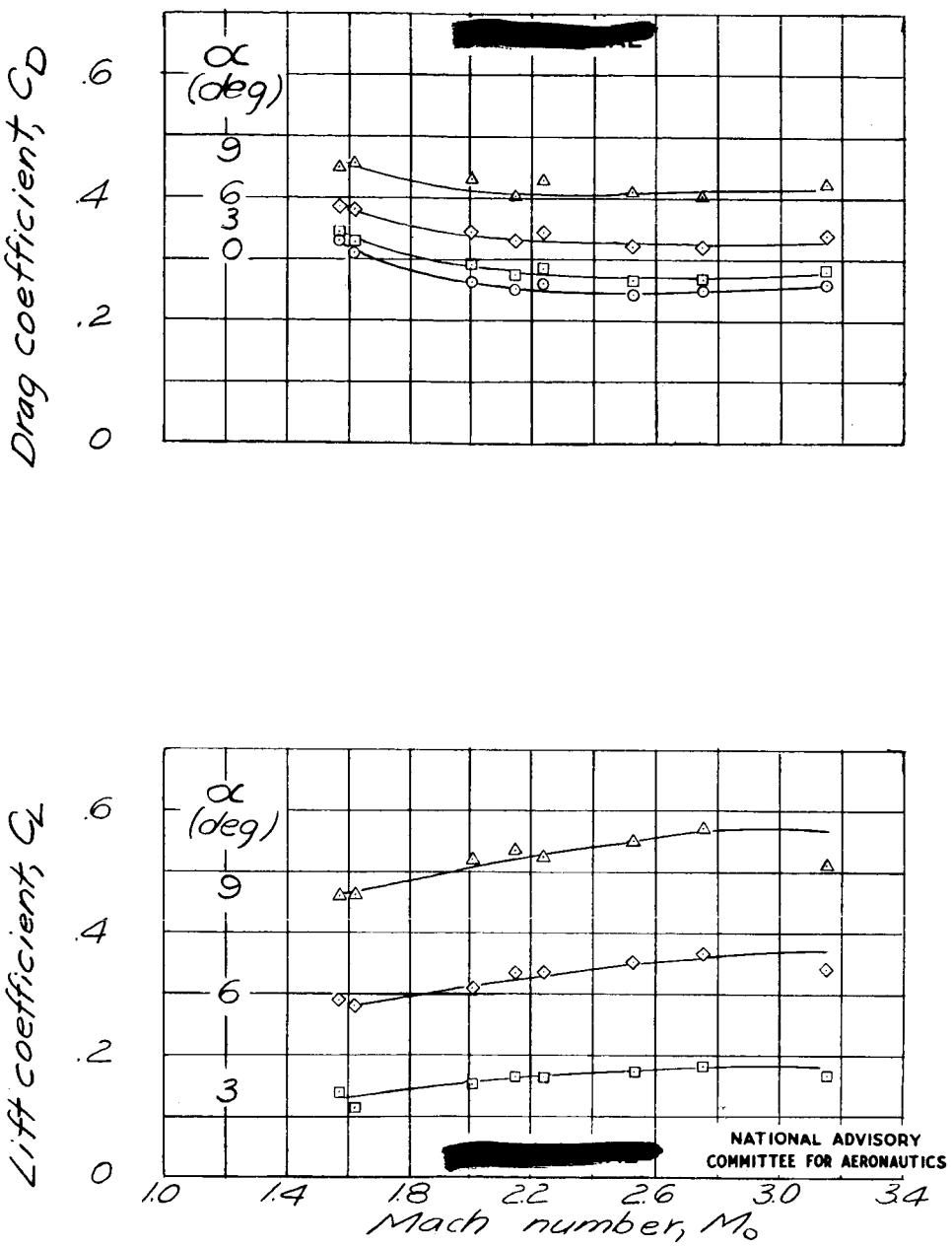

Figure 19.- Lift, drag, and moment coefficients and position of center of pressure as functions of Mach number for various angles of attack. Model 10. (Göttingen)

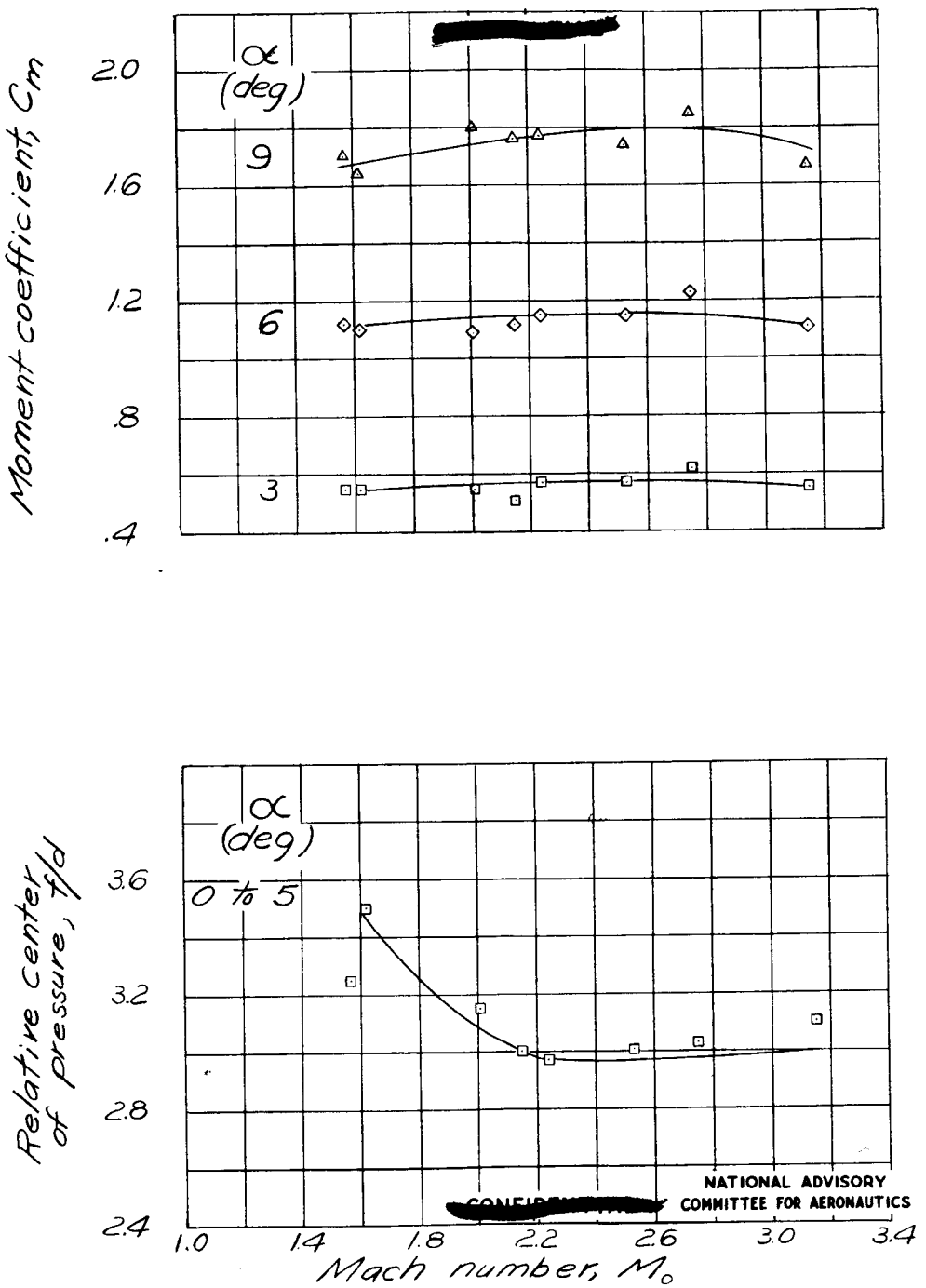

Figure 19.- Concluded.

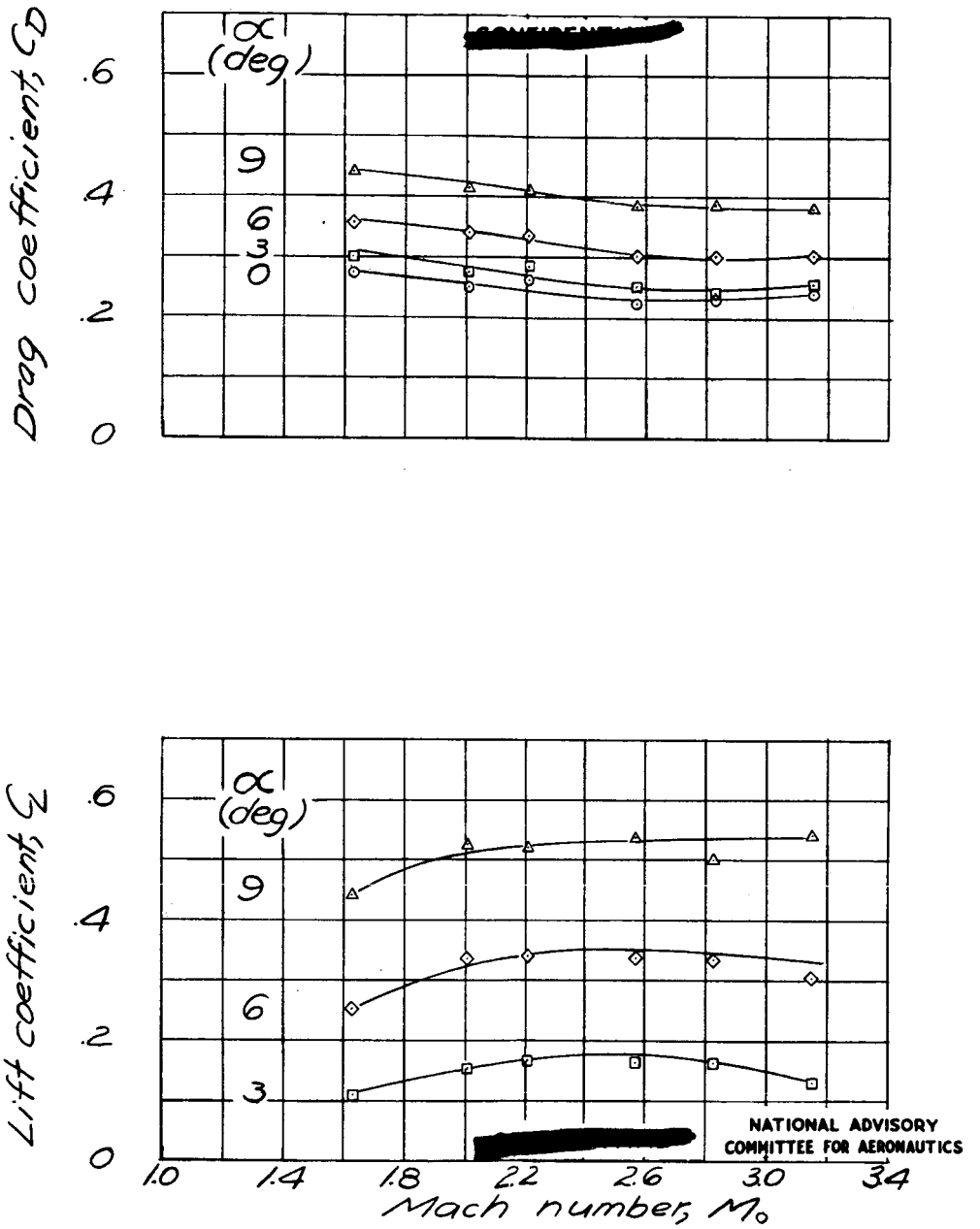

Figure 20.- Lift, drag, and moment coefficients and position of center of pressure as functions of Mach number for various angles of attack. Model 11. (Göttingen)

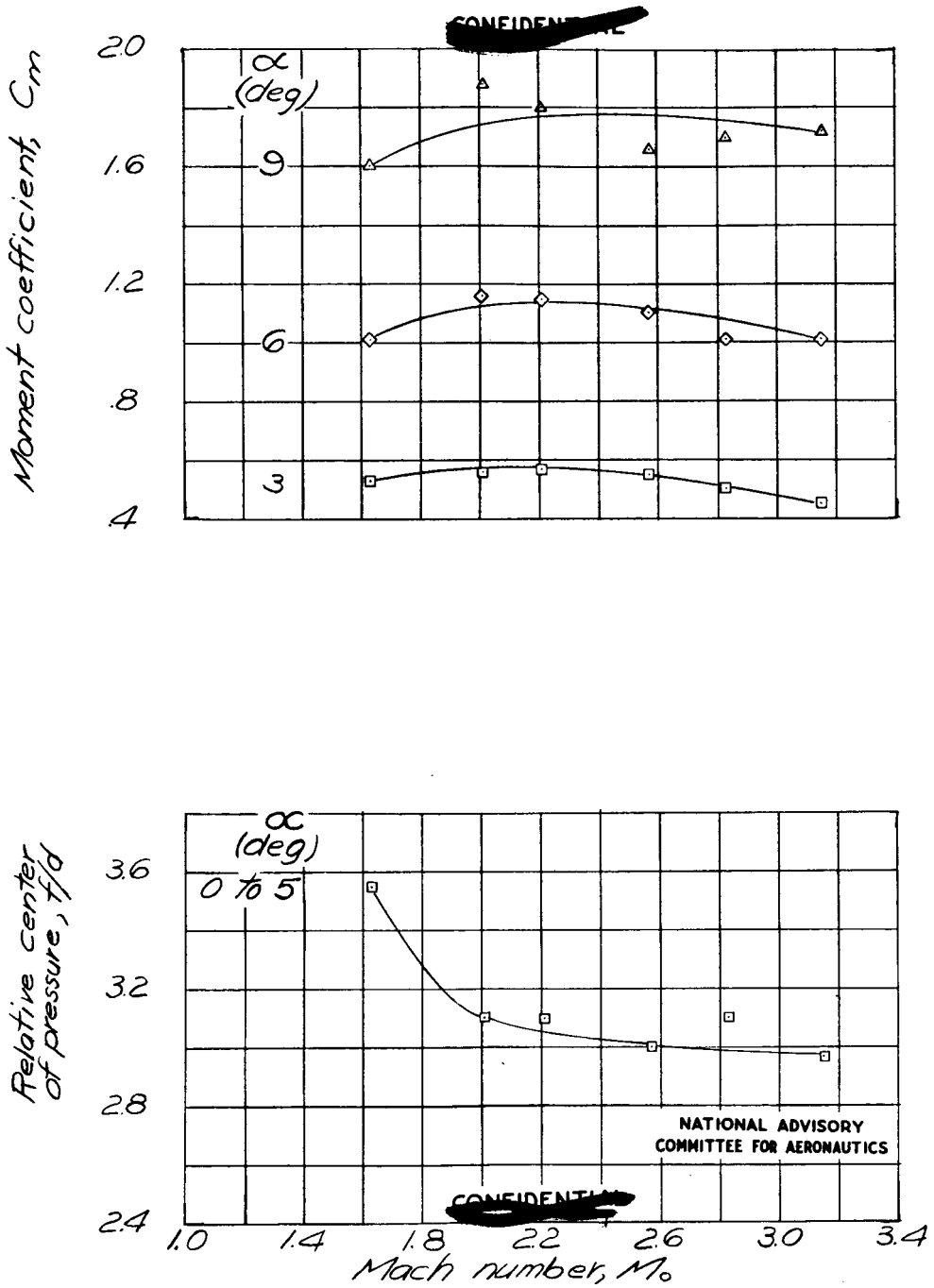

Figure 20.- Concluded.

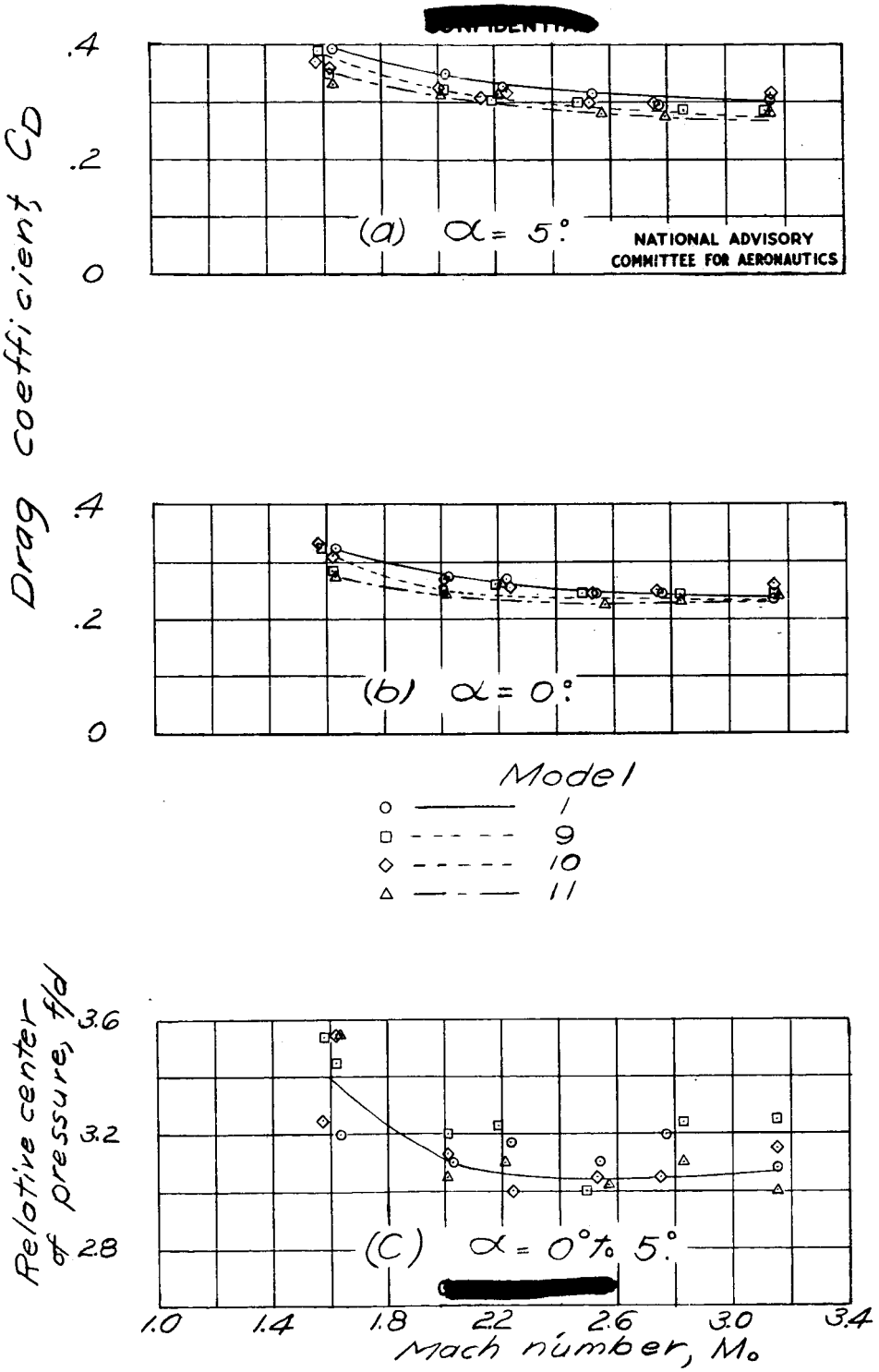

Figure 21.- Drag coefficient and relative center of pressure as functions of Mach number. Models 1, 9, 10, and 11. (Göttingen)

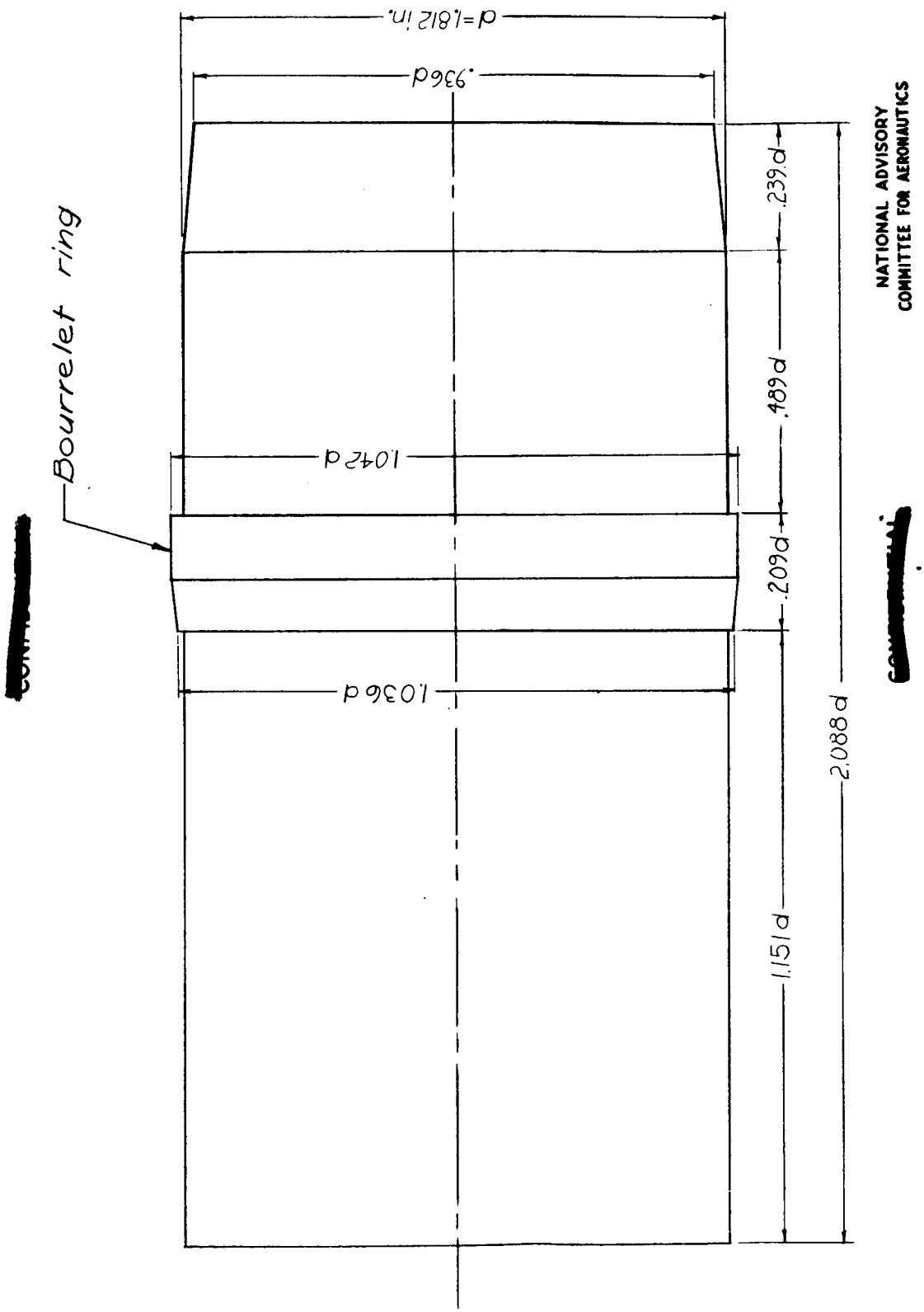

Figure 22.- The body of the projectiles tested at Guidonia.

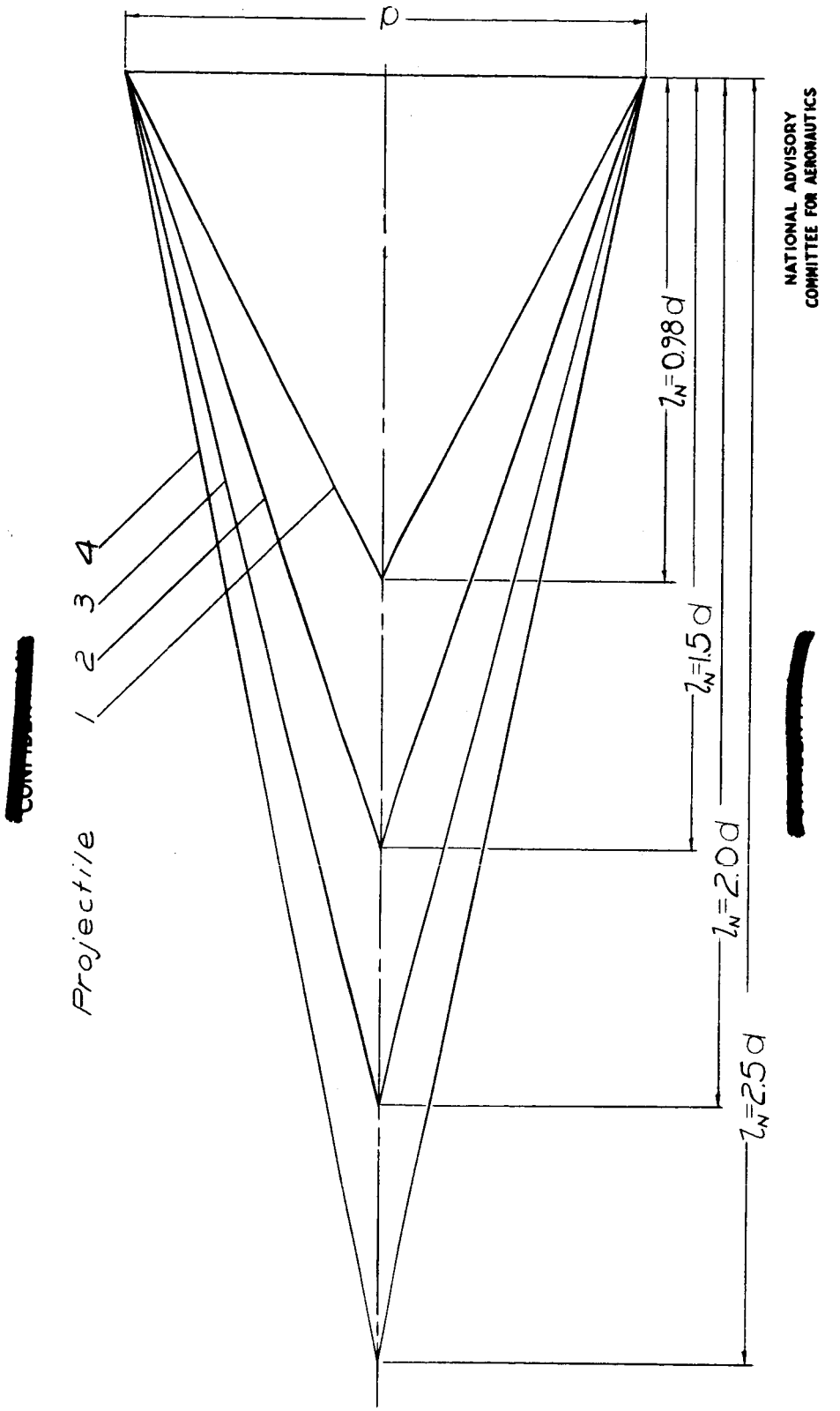

Figure 23.- The noses of the projectiles tested at Guidonia.

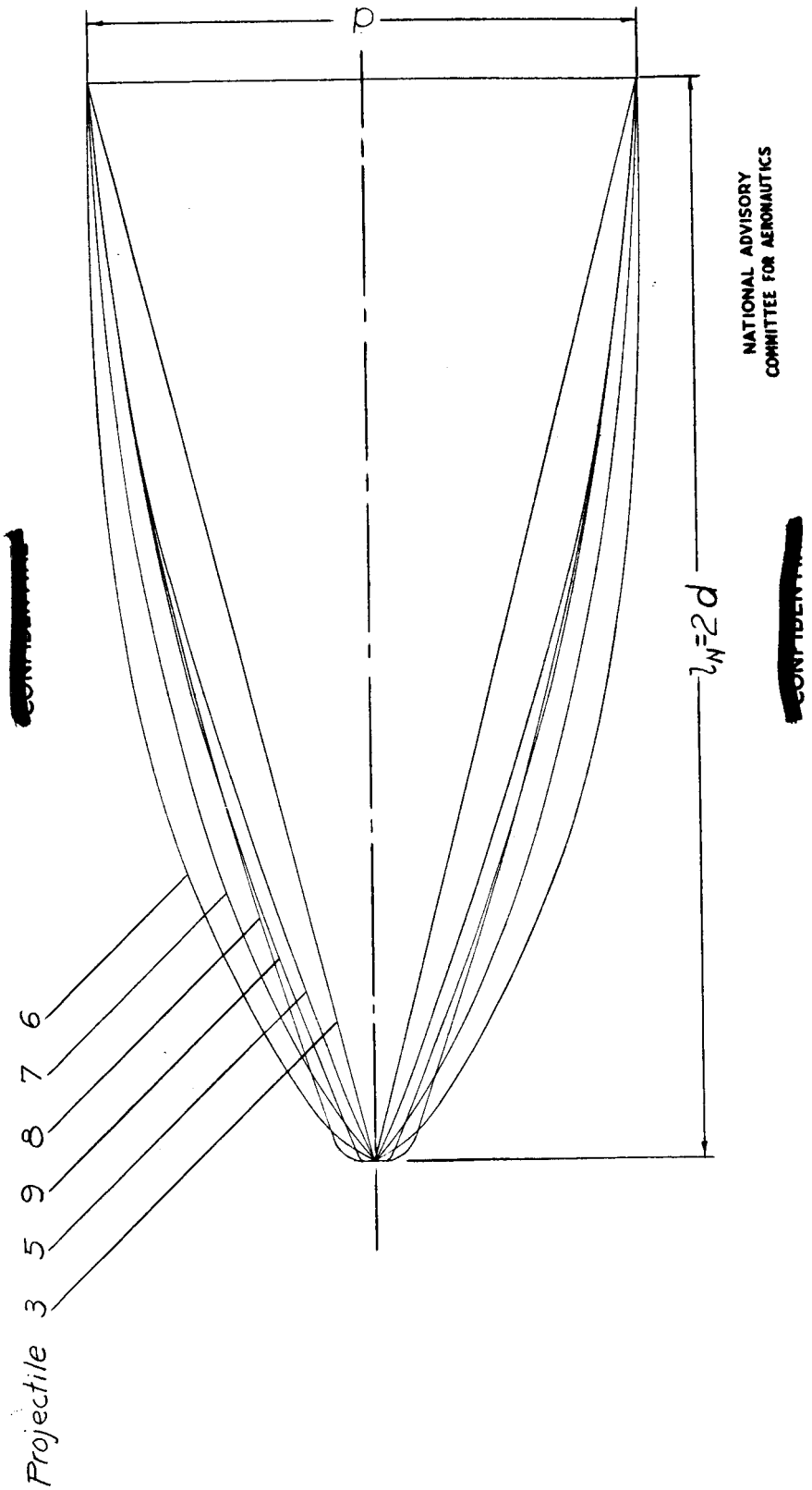

Figure 23.- Concluded.

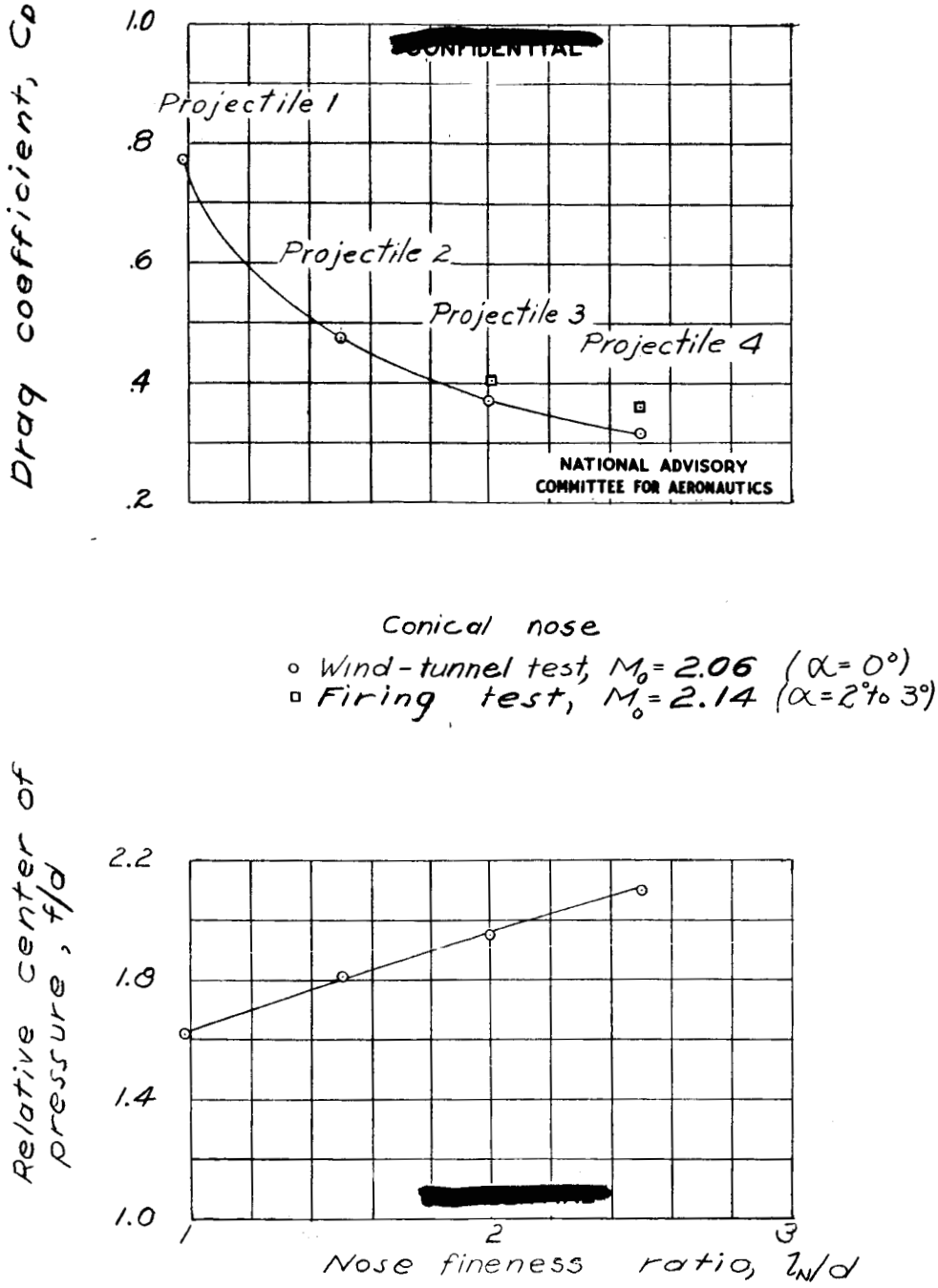

Figure 24.- Variation of drag coefficient and relative center of pressure with fineness ratio of nose. $\alpha = 0°$. (Guidonia)

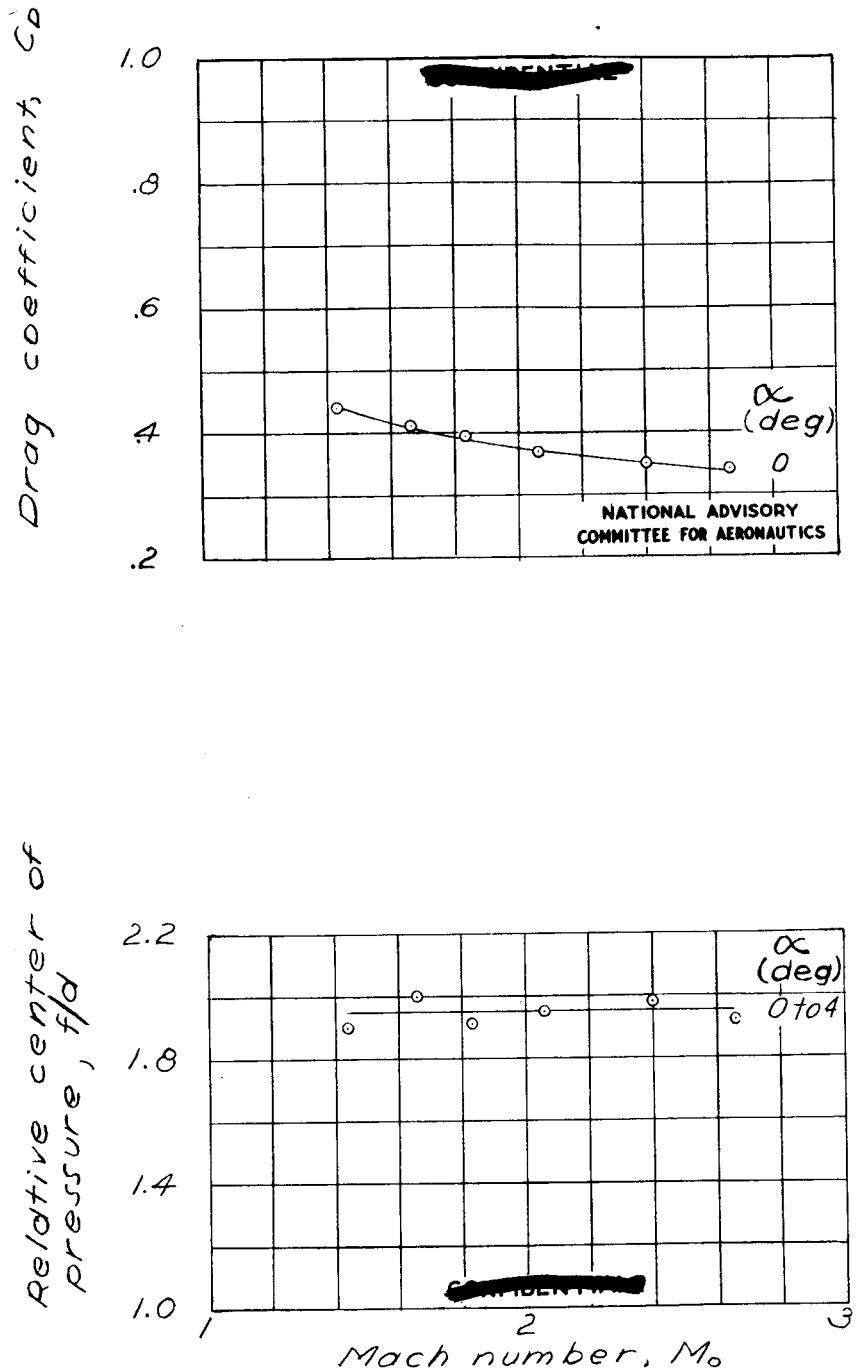

Figure 25.- Variation of drag coefficient and relative center of pressure with Mach number for projectile 3. (Guidonia)

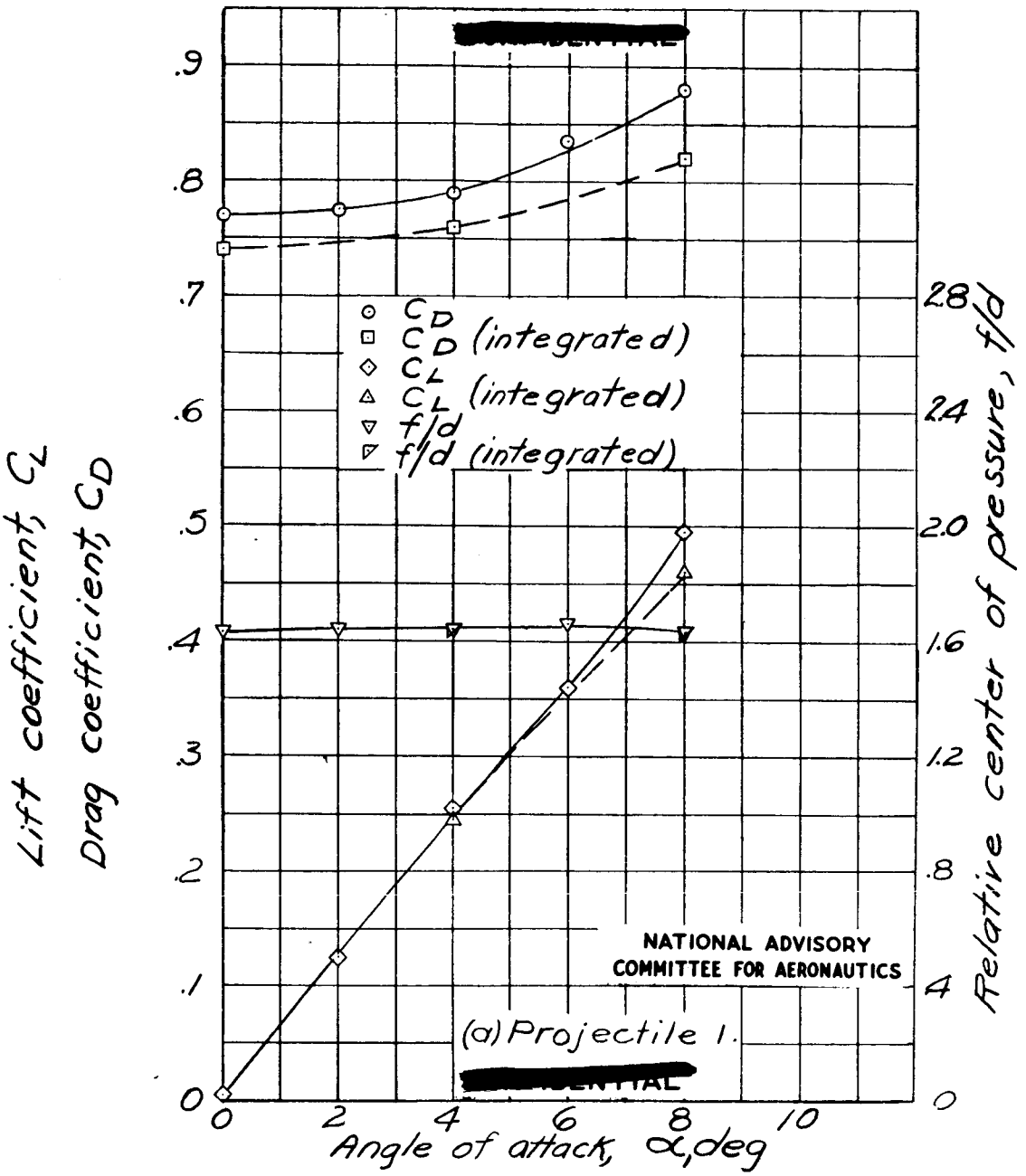

Figure 26.- Variation of the aerodynamic coefficients with angle of attack for projectiles 1 and 3. M_o = 2.06. (Guidonia)

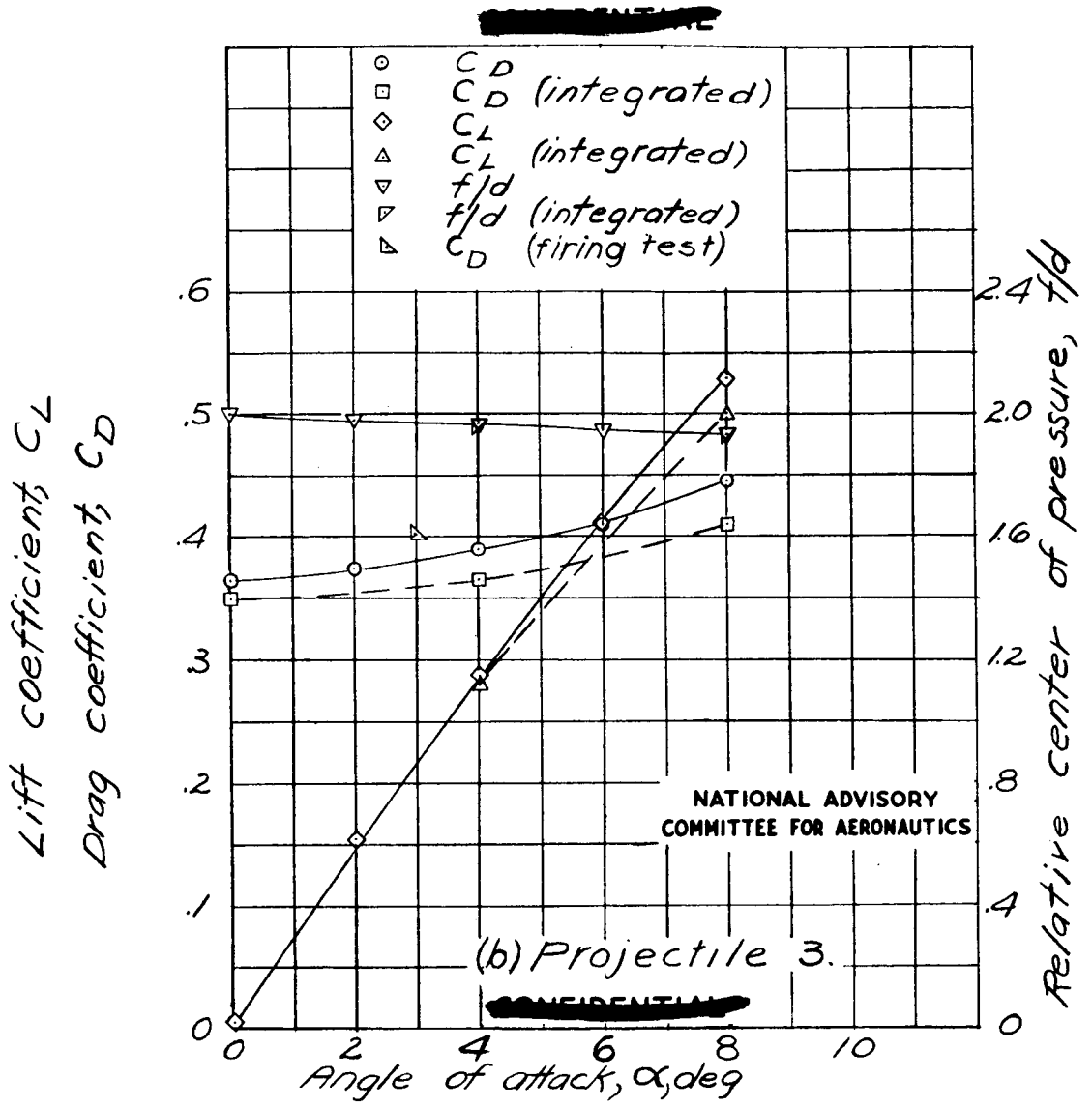

Figure 26.- Concluded.

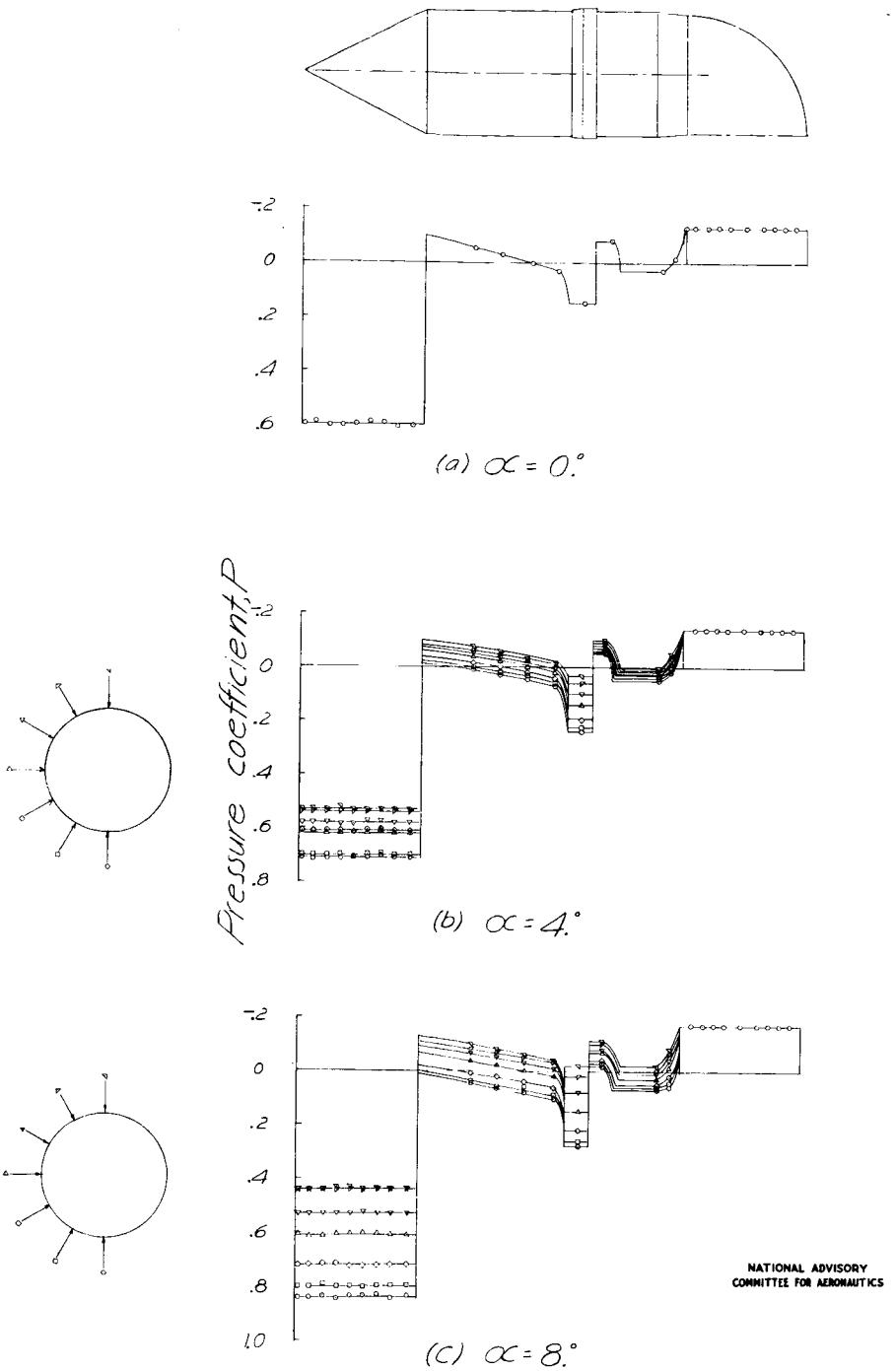

Figure 27. - Pressure distributions on projectile 1. All points on rear face of projectile are approximately the same. $M_o = 2.06$. (Guidonia)

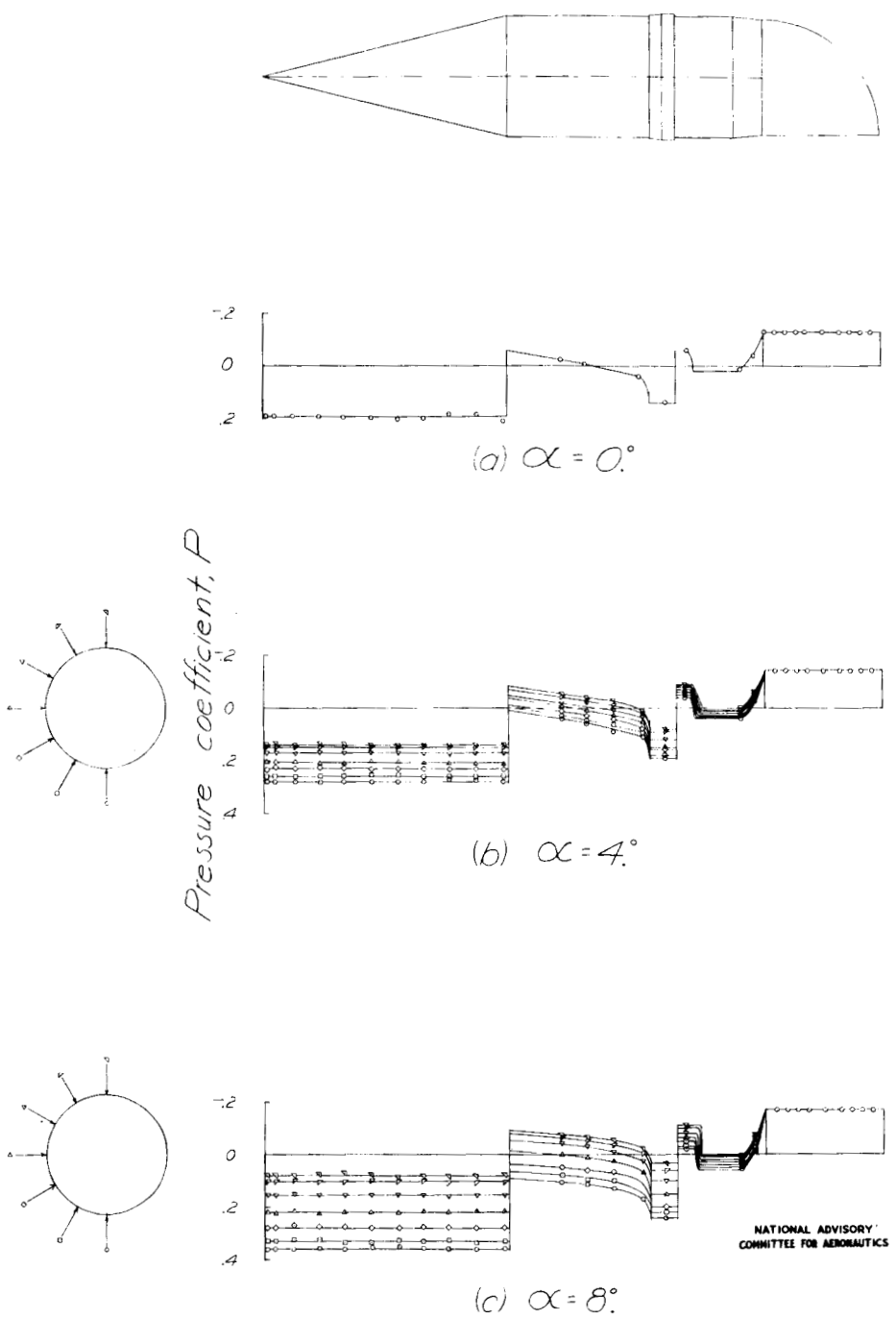

Figure 28.- Pressure distributions on projectile 3. All points on rear face of projectile are approximately the same. M_o = 2.06. (Guidonia)

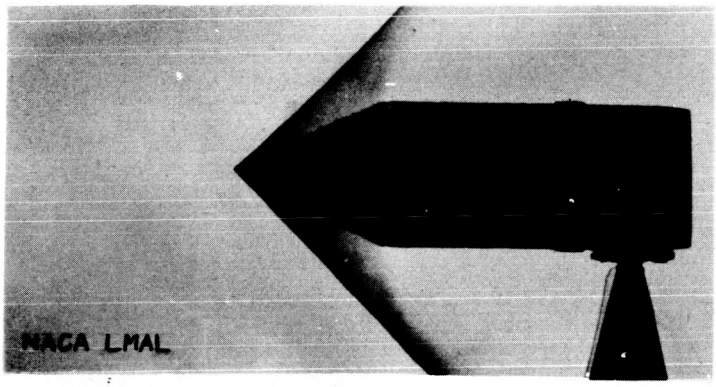

(a) Projectile 1.

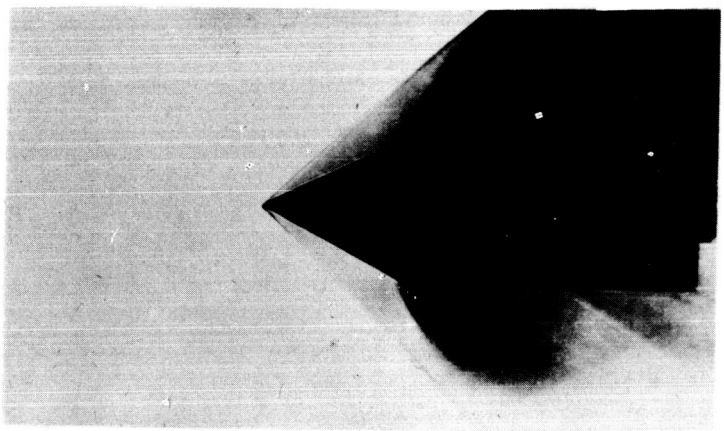

(b) Projectile 1.

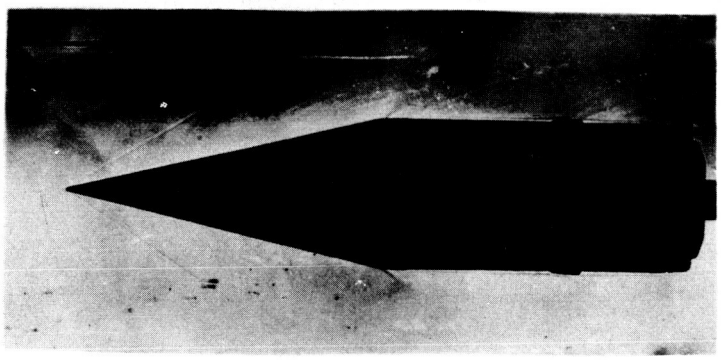

(c) Projectile 3.

Figure 29.- Optical data taken by schlieren apparatus for projectiles 1 and 3. $\alpha = 0^{\circ}$: $M_{\infty} = 2.06$. (Guidonia)

NATIONAL ADVISORY COMMITTEE FOR AERONAUTICS
LANGLEY MEMORIAL AERONAUTICAL LABORATORY - LANGLEY FIELD, VA.

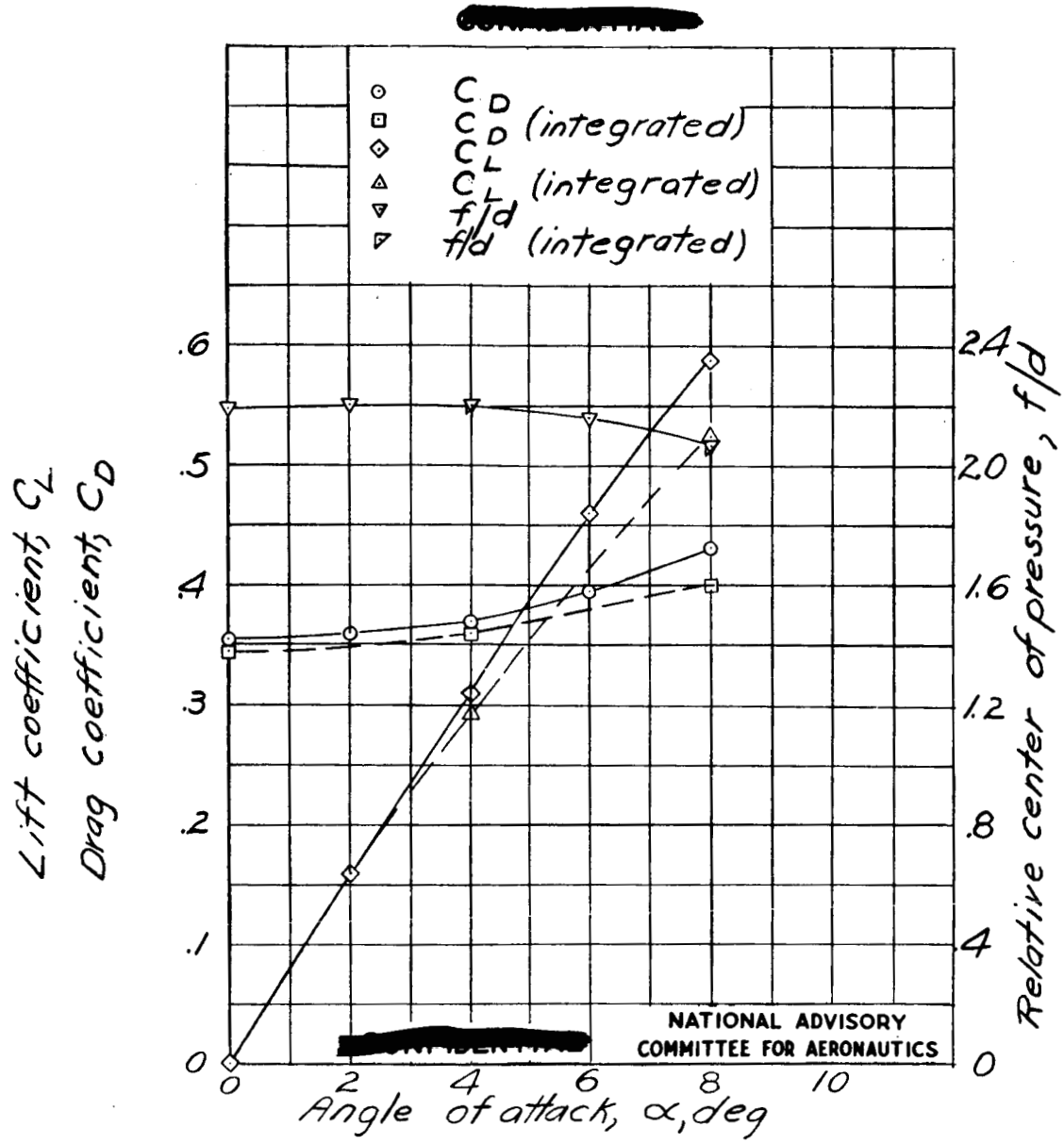

Figure 30.- Variation of the aerodynamic coefficients with angle of attack for projectile 8. M_o = 2.06. (Guidonia)

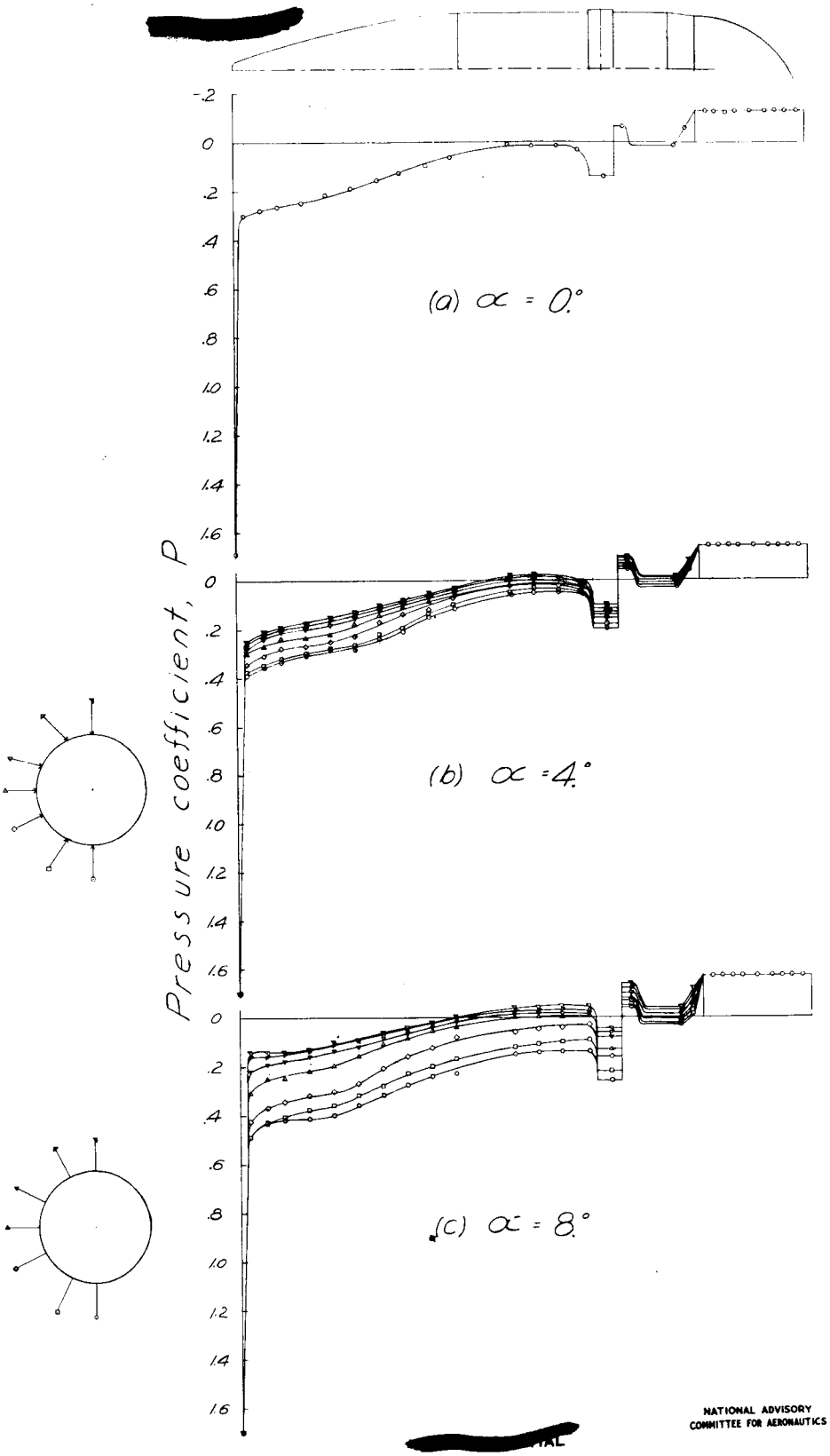

Figure 31.- Pressure distributions on projectile 8. All points on rear face of projectile are approximately the same. M_o = 2.06. (Guidonia)

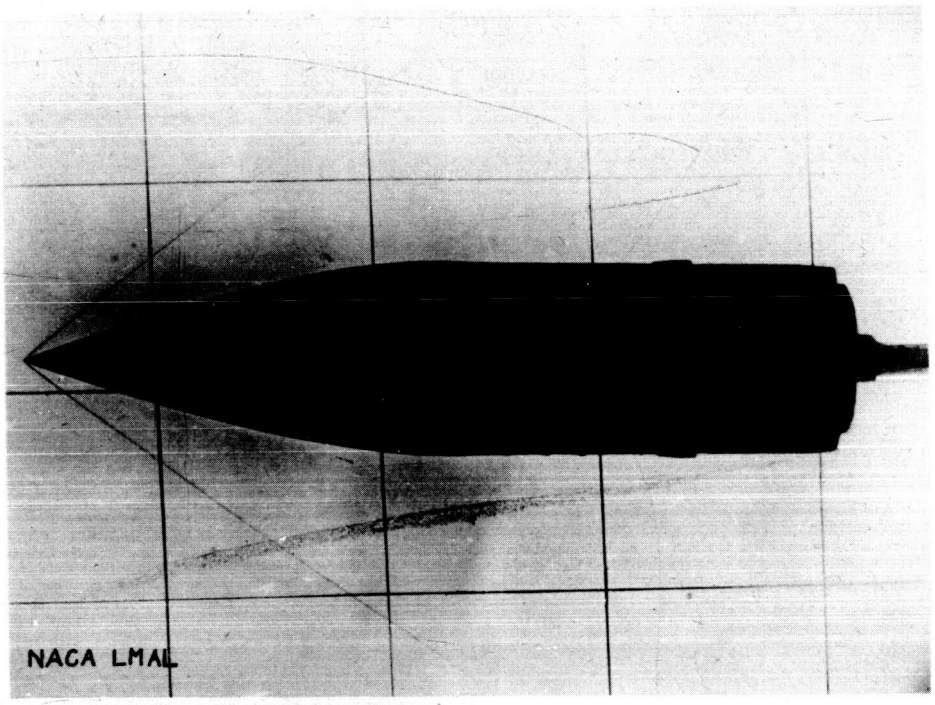

(a) Taken by shadowgraph apparatus.

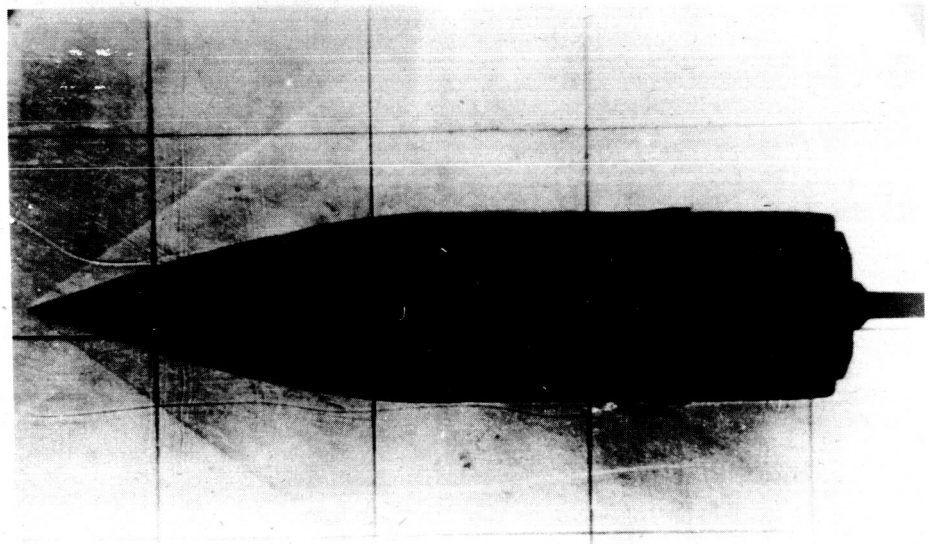

(b) Taken by schlieren apparatus.

Figure 32.- Optical data for projectile 5. $\alpha = 0^{\circ}$; $M_o = 2.06$. (Guidonia)

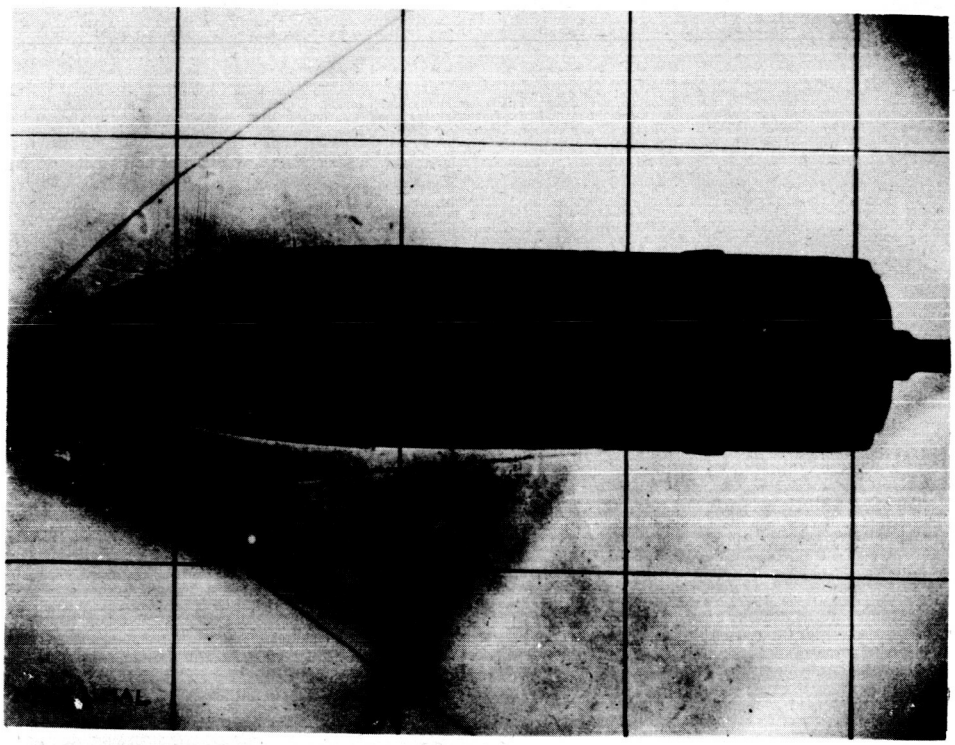

(a) Taken by shadowgraph apparatus.

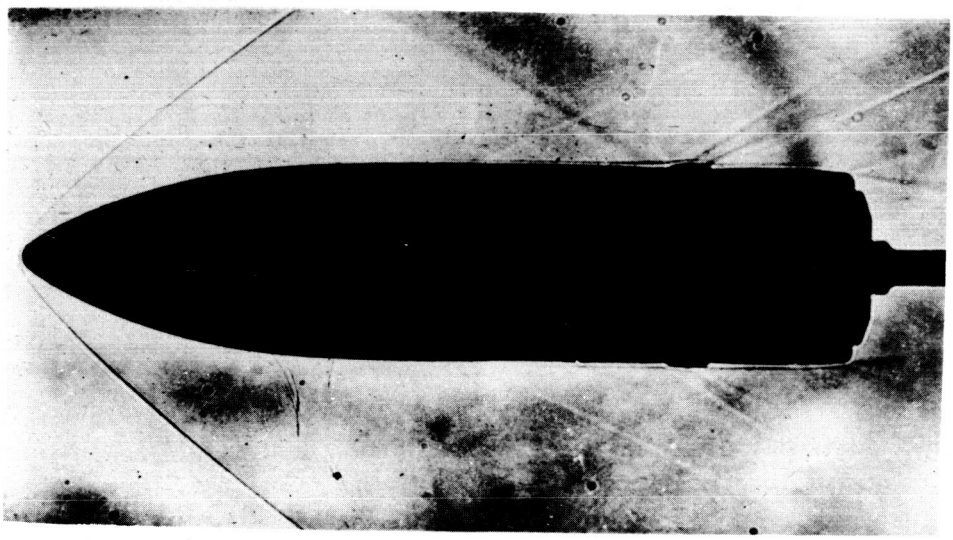

(b) Taken by schlieren apparatus.

Figure 33.- Optical data for projectile 6. $\alpha = 0^{\circ}$; $M_0 = 2.06$. (Guidonia)

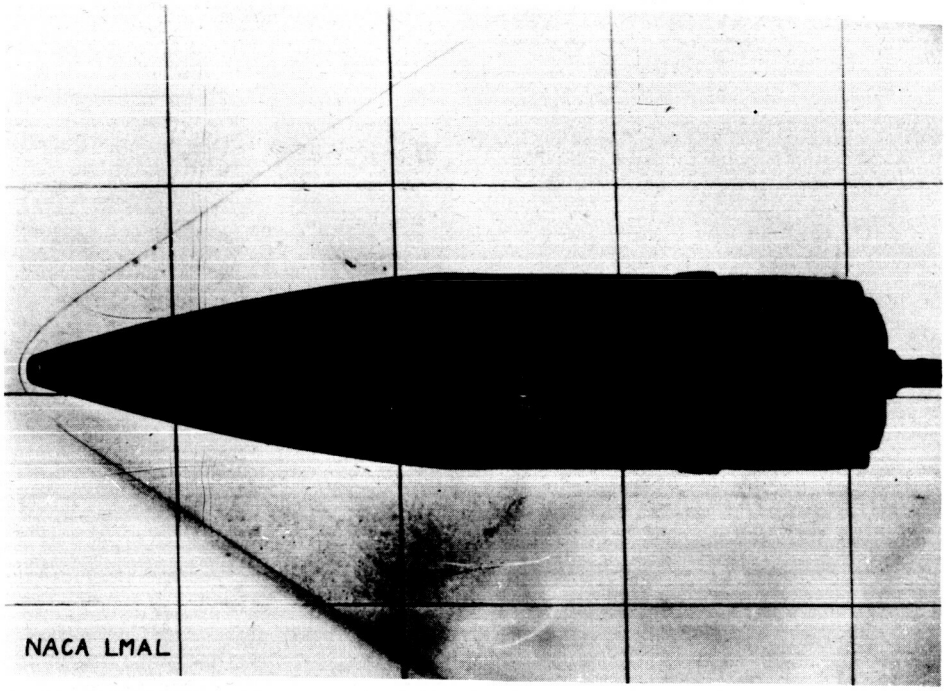

(a) Taken by shadowgraph apparatus.

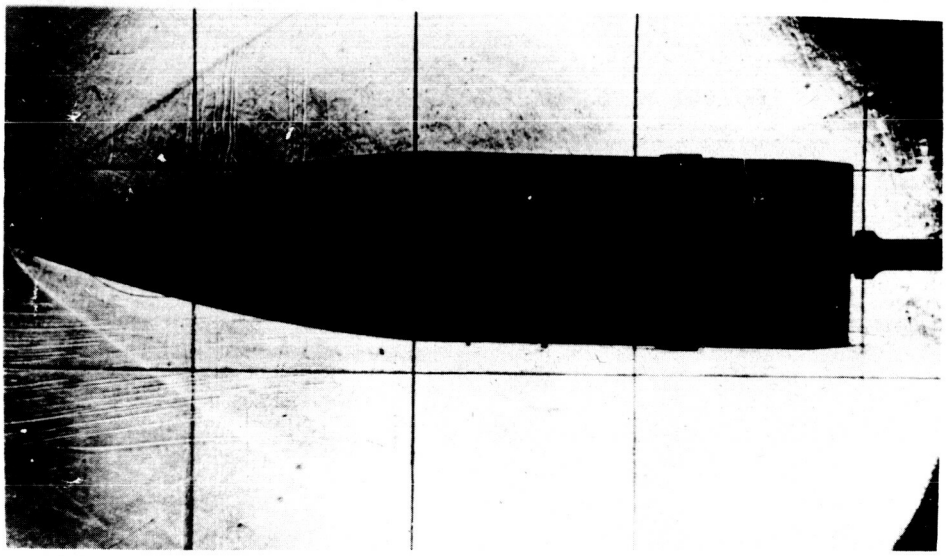

(b) Taken by schlieren apparatus.

Figure 34.- Optical data for projectile 8. $\alpha = 0^{\circ}$; $M_0 = 2.06$. (Guidonia)

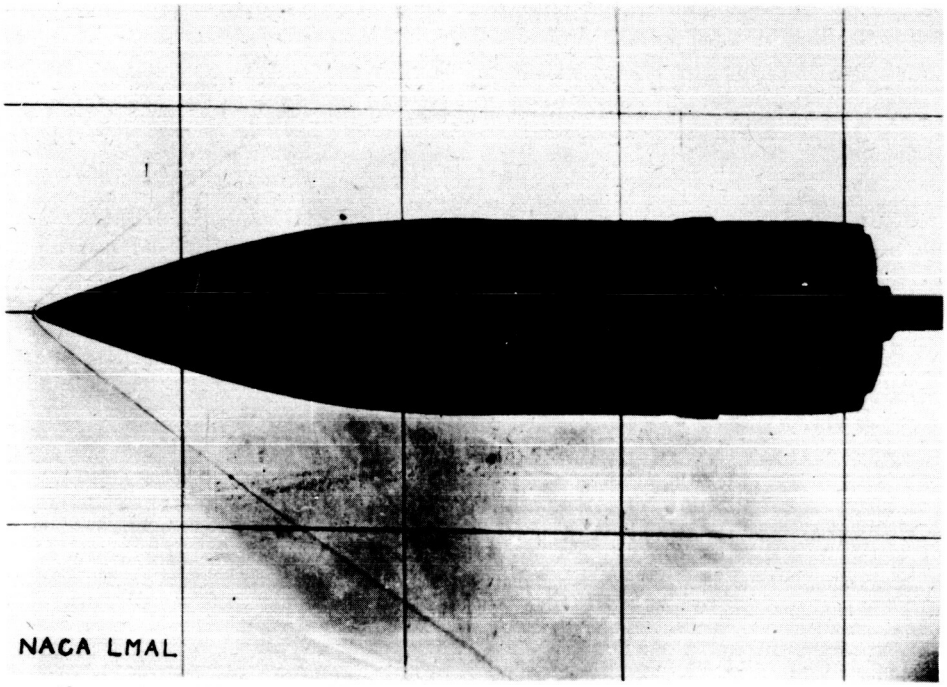

(a) Taken by shadowgraph apparatus.

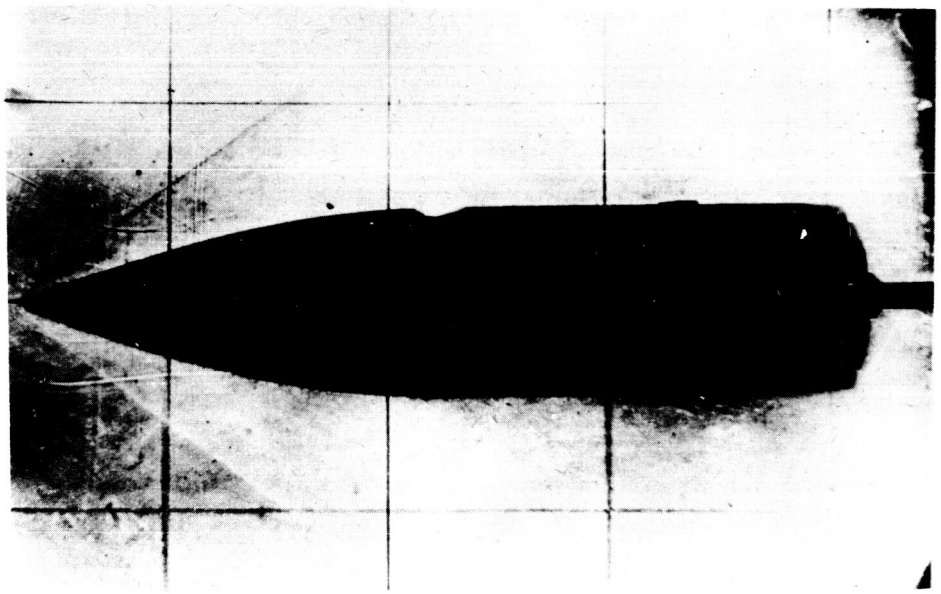

(b) Taken by schlieren apparatus.

Figure 35.- Optical data for projectile 9. $\alpha = 0^{o}$; $M_{o} = 2.06$. (Guidonia)